

26/1/52

# ON THE SCATTERING MATRIX OF SYMMETRICAL WAVEGUIDE JUNCTIONS

## *PROEFSCHRIFT*

TER VERKRIJVING VAN DE GRAAD VAN  
DOCTOR IN DE TECHNISCHE WETENSCHAP  
AAN DE TECHNISCHE HOGESCHOOL TE  
DELFT, OP GEZAG VAN DE RECTOR MAG-  
NIFICUS, Dr O. BOTTEMA, HOOGLERAAR  
IN DE AFDELING DER ALGEMENE WETEN-  
SCHAPPEN, VOOR EEN COMMISSIE UIT DE  
SENAAT TE VERDEDIGEN OP WOENSDAG  
27 FEBRUARI 1952, DES NAMIDDAGS TE 4 UUR

DOOR

ANTON EDUARD PANNENBORG  
NATUURKUNDIG INGENIEUR  
GEBOREN TE 's-GRAVENHAGE



10123070

Dit proefschrift is goedgekeurd door de promotor  
Prof. Dr R. Kronig

## CONTENTS

	page
INTRODUCTION . . . . .	7
Chap. I. FUNDAMENTAL THEOREMS . . . . .	9
I. 1. General remarks . . . . .	9
I. 2. Fields in waveguides . . . . .	10
I. 3. Scattering matrix . . . . .	11
I. 4. Shift in position of terminal reference planes . . . . .	12
I. 5. Symmetry of the scattering matrix . . . . .	13
I. 6. Lossless junctions . . . . .	14
I. 7. Frequency dependence of a unitary scattering matrix . .	15
Chap. II. RESONATORS . . . . .	18
II. 1. Quality factor . . . . .	18
II. 2. Fundamental considerations . . . . .	10
II. 3. Resonators with one output lead . . . . .	21
II. 4. Resonators with two output leads . . . . .	26
II. 5. Losses in the output circuit . . . . .	30
Chap. III. SYMMETRY ANALYSIS OF WAVEGUIDE JUNCTIONS . . . . .	32
III. 1. Representation of a symmetry group . . . . .	32
III. 2. Relation between the symmetry of a junction and its scattering matrix . . . . .	34
III. 3. Field distribution in a symmetry plane . . . . .	38
Chap. IV. JUNCTIONS OF FOUR WAVEGUIDES WITH TWO-FOLD PLANAR SYMMETRY . . . . .	40
IV. 1. The general case . . . . .	40
IV. 2. The nature of the solution . . . . .	44
IV. 3. The degenerate case . . . . .	44
IV. 4. The wave matrix . . . . .	47
IV. 5. Shift of the reference planes . . . . .	50
Chap. V. DIRECTIONAL COUPLERS . . . . .	51
V. 1. Condition for perfect directivity . . . . .	51
V. 2. Bethe-hole coupler . . . . .	52
V. 3. Systems of identical junctions connected in cascade .	53
V. 4. Frequency dependence of directional couplers . . . .	60
V. 5. Variable attenuator . . . . .	62
V. 6. Standard matching transformer . . . . .	65
Chap. VI. RESONANT SLOTS . . . . .	71
VI. 1. Single slots . . . . .	71
VI. 2. Measurements on single slots . . . . .	76
VI. 3. Resonant directional coupler . . . . .	80

## INTRODUCTION

The physical configuration of microwave circuits is in all but the simplest cases too intricate to enable one to solve Maxwell's equations subject to the boundary conditions imposed. For practical purposes, however, it is not necessary to know explicitly the components of the electromagnetic field at every point of the interior of the structure. It often suffices to know how the structure affects the field in the leads connecting it to the outside.

This approach to the behaviour of microwave circuits, sometimes called transducer theory, has been made up till now in the majority of cases with the aid of equivalent circuits. It has proved itself to be a powerful tool for the analysis of waveguide junctions. The physical insight so obtained is very illuminating, especially for the radio engineer accustomed to low-frequency lumped-circuit concepts.

On the other hand for structures with more than two or three output leads the equivalent circuit merely serves to provide a well-defined framework in which numerical values obtained from experiments can be inserted. In these more intricate cases the value of the representation as a guide to better understanding seems at least doubtful; anyway much of the charm of the method is lost. The way out of this difficulty is found in an alternative method, where the description of the field in the output leads of a junction is made by specifying not the ratios of electric and magnetic components, but rather the ratios of amplitudes of travelling waves incident on and emergent from the junction. In analogy with other branches of physics the matrix expressing the relation between these wave amplitudes is called the *scattering matrix* of the junction. Up till now the scattering matrix has been used to a limited extent only and — for the reasons stated above — especially in the case of junctions with more than two output leads.

Apart from the general theorems supplied to transducer theory by Maxwell's equations, a source of information is often available in the form of the symmetries pertaining to the structure under consideration. In very simple cases the consequences of symmetry can be found by inspection. For more intricate situations a formalism has been developed by Dicke<sup>1</sup>); it introduces symmetry operators, subject to which the solution of Maxwell's equations must remain invariant. In this way it sometimes becomes possible to construct a number of special solutions, the most general solution then being a linear combination of these. The number of parameters needed to specify the behaviour of a junction can thus be considerably reduced. For the symmetrical structures with many output leads, where the formalism is most useful, the scattering matrix is preferable

to impedance or admittance representations. Therefore the symmetry formalism usually is applied to the former method.

As stated above, the scattering matrix has found little application for simple circuits. Especially in the case of resonators the impedance or admittance description has been used almost exclusively. This is quite logical from a historical point of view as work in the microwave range originates from a gradual extension of techniques well known for longer wavelengths. In this way it was natural to transfer the familiar concept of an LCR circuit to microwave resonators. That this procedure is quite correct was proved subsequently by several authors, e.g. by Slater<sup>2)</sup>.

On the other hand Tomonaga<sup>3)</sup> has shown how the scattering matrix can be used equally well for the description of the behaviour of resonators. The results are, of course, identical with those from calculations on an impedance basis and whilst to the radio engineer the simple LCR representation for a resonator is very attractive, the scattering description should appeal for analogous reasons to the physicist. Furthermore the latter method seems to involve slightly less specific assumptions about the nature of the resonant structure.

In Chap. I a short recapitulation is given of the fundamental properties of the scattering matrix. This seems justified since elsewhere in literature<sup>1),4)</sup> the theorems are derived, using almost invariably the impedance matrix as an intermediate station. Chapter II contains a slight extension of Tomonaga's theory together with some examples demonstrating the practical usefulness of this theory. Chapter III gives an outline of the symmetry formalism. In Chap. IV the general properties of structures with four output leads having a high degree of symmetry are derived. In Chap. V these results are applied to waveguide systems with special reference to directional couplers, while finally Chap. VI deals with analogous systems incorporating resonant elements.

## CHAPTER I. FUNDAMENTAL THEOREMS

### I. 1. General remarks

As in the following pages we shall be concerned with certain applications of transducer theory to microwave structures and as these investigations will be carried out with the aid of the scattering matrix, it seems proper to start with the derivation of some fundamental properties of this matrix. Because extensive demonstrations constituting the rigorous foundation of transducer theory can be found elsewhere<sup>1),4)</sup>, we will confine ourselves to a recapitulation of those proofs that are of direct importance for the contents of the following chapters. In this connection it is supposed that the reader is familiar with waveguide theory.

Before embarking on the subject we will state some conventions and restrictions that will be adhered to throughout.

- (i) The time factor is understood to be  $e^{-i\omega t}$ . Unless specifically stated otherwise  $\omega$  is real and the fields vary harmonically with time.
- (ii) All structures considered are linear and passive. Anisotropic media are allowed with the limitation that the tensors describing their permittivity, permeability and conductivity must be symmetrical.
- (iii) It is possible to surround a structure by a closed surface of finite dimensions on which all field quantities are zero except where this surface cuts the output leads.
- (iv) The leads, in which the terminal fields relating to a structure are defined, consist of ideal (i.e. lossless and cylindrical) waveguides, not containing anisotropic materials.
- (v) In each output lead power is transported by one mode only.
- (vi) Terminal surfaces are drawn at sufficient distance from any discontinuity so that the effect of non-propagating modes can be ignored.
- (vii) Rationalized MKS(Giorgi) units are used.

Some points need some comment. Condition (iii) merely requires that the structure and its output leads are effectively shielded. Point (v) constitutes no important restriction. In fact, because of the orthogonality properties of the characteristic solutions (called modes) of Maxwell's equations for an ideal waveguide, a system of two modes in one waveguide is within the formalism of transducer theory fully equivalent to a system of two modes each in a different waveguide. Point (vi), finally, is only of significance when the interconnection between two transducers is considered. It states that the connecting leads should be sufficiently long to prevent non-propagating modes excited in the interior of one transducer from reaching any discontinuity in the interior of the other transducer. If this condition is not fulfilled, the behaviour of the combination of two structures cannot be accurately predicted from the transducer data of the separate

structures. Indeed, it should always be remembered that transducer theory combined with the necessary experiments gives for most applications sufficient, but never complete information on the repartition of the electromagnetic field.

As a consequence of points (i), (ii), and (vii) Maxwell's equations have the form

$$\begin{aligned} \operatorname{curl} \mathbf{H} &= (-i\omega\epsilon + \sigma) \mathbf{E}, \\ \operatorname{curl} \mathbf{E} &= i\omega\mu\mathbf{H}, \end{aligned} \quad \left. \right\} \quad (1)$$

the permittivity  $\epsilon$ , the permeability  $\mu$  and the conductivity  $\sigma$  being independent of time and of the field vectors.

## I. 2. Fields in waveguides

We next recall without proof some results from waveguide theory as far as they are needed in later sections.

Let the  $z$ -axis be parallel to the axis of the waveguide. The general expressions for the electric and magnetic fields of a waveguide mode can be written as follows<sup>2)</sup>:

$$\begin{aligned} \mathbf{E} &= \mathbf{E}_t(a e^{-i\beta z} + b e^{i\beta z}) + \mathbf{k} E_z(a e^{-i\beta z} - b e^{i\beta z}), \\ \mathbf{H} &= \mathbf{H}_t(a e^{-i\beta z} - b e^{i\beta z}) + \mathbf{k} H_z(a e^{-i\beta z} + b e^{i\beta z}). \end{aligned} \quad \left. \right\} \quad (2)$$

Here  $E_z$  and  $H_z$  are the longitudinal components;  $\mathbf{k}$  represents the unit vector in the positive  $z$ -direction. The transverse components  $\mathbf{E}_t$  and  $\mathbf{H}_t$  are vector functions (derivable from  $E_z$  and  $H_z$ ) lying in a plane perpendicular to the  $z$ -axis;  $a$  and  $b$  are amplitude coefficients for the waves in the negative and the positive  $z$ -direction respectively. The propagation constant  $\beta$  is real for propagating modes. As the  $z$ -dependence has been written explicitly in eqs (2), the quantities  $E_z$ ,  $H_z$ ,  $\mathbf{E}_t$  and  $\mathbf{H}_t$  are functions of the transverse coordinates only.

Equations (2) are valid for all three classes of modes: transverse electromagnetic or TEM( $E_z = 0$ ,  $H_z = 0$ ), transverse electric or TE( $E_z = 0$ ) and transverse magnetic or TM( $H_z = 0$ ).

The transverse electric and magnetic fields are proportional to each other; the relation is

$$\mathbf{E}_t = Z_0 (\mathbf{k} \times \mathbf{H}_t), \quad (3)$$

where  $Z_0$  is a constant which is real for propagating modes.

If a section of waveguide for which the field components are given by eqs (2) is fed by a generator sending power in the negative  $z$ -direction, where the guide is terminated by a passive load, it is natural to define a reflection coefficient as the ratio of the amplitudes of the waves incident on and reflected by the load. As the transverse electric field is most easily

accessible to measurement, we base the definition on this component; the reflection coefficient  $\Gamma$  thus derived from eqs (2) is

$$\Gamma = \frac{b e^{i\beta z}}{a e^{-i\beta z}} = \frac{b}{a} e^{2i\beta z}. \quad (4)$$

To determine the expression for power flow, first the  $z$ -component of the time average Poynting vector  $S$  is formed, viz.

$$S_z = \frac{1}{4} \mathbf{k}(\mathbf{E} \times \mathbf{H}^* + \mathbf{E}^* \times \mathbf{H}). \quad (5)$$

The asterisk denotes the complex conjugate. Substituting eqs (2) and (3) in eq. (5) it is clear that only the transverse field components contribute to  $S_z$ :

$$S_z = \frac{|E_t|^2}{2Z_0} \langle |b|^2 - |a|^2 \rangle = \frac{1}{2} Z_0 |H_t|^2 \langle |b|^2 - |a|^2 \rangle. \quad (6)$$

The power flow  $P$  in the positive  $z$ -direction is obtained by integrating  $S_z$  over the cross section  $\Omega$  of the guide. But first we introduce the normalization condition. The expression for power flow is brought into its most simple form by putting

$$\frac{1}{Z_0} \int_{\Omega} |E_t|^2 d\Omega = Z_0 \int_{\Omega} |H_t|^2 d\Omega = 1. \quad (7)$$

With this condition  $P$  becomes

$$P = \frac{1}{2} \langle |b|^2 - |a|^2 \rangle. \quad (8)$$

When applying eq. (8) to the setup with generator and load as used for deriving eq. (4) it is to be noted that it represents the power flow from the load towards the generator.

### I. 3. Scattering matrix

Consider a waveguide junction subject to the conditions stated in Sec. 1. In each of the  $N$  output leads a coordinate system is introduced, the  $z$ -axis being parallel to the axis of the waveguide and pointing outward from the junction. The electromagnetic field in each lead can be written in the form of eqs (2), indicating the presence in output lead ( $n$ ) of an incident wave of amplitude  $a_n$  and an outgoing wave of amplitude  $b_n$ . The linearity of Maxwell's equations together with condition (ii), Sec. 1, requires that the amplitudes  $b_n$  of the outgoing waves are linear functions of the amplitudes  $a_n$  of the incident waves. Grouping the quantities  $a_n$  and  $b_n$  together in column matrices  $A$  and  $B$  respectively, this linear relation can be formally represented by

$$B = SA, \quad (9)$$

the elements of the *scattering matrix*  $S$  being independent of the amplitudes,  $a_n$  and  $b_n$  and of time.

The physical meaning of the elements of  $S$  is closely related to the reflection coefficient  $\Gamma$  introduced in eq. (4). In fact, applying eq. (9) to the case of a structure with only one lead, i.e. a waveguide terminated by a load, the single remaining element of  $S$  is seen to be identical with  $\Gamma(z = 0)$ . In the general case with  $N$  output leads the diagonal elements of the square matrix  $S$  of order  $N$  relate outgoing waves to waves incident in the same lead; they are of the same nature as a reflection coefficient. The off-diagonal elements, relating the outgoing wave in one lead to waves incident in other leads, may be called transmission coefficients.

If we put all  $a_n$  equal to zero except  $a_m$ , which situation is in practice achieved by connecting a generator to lead ( $m$ ), all other leads being terminated by a matched load, and choose  $a_m$  equal to 1, the elements of the  $m$ 'th column of  $S$  give the amplitudes of the outgoing waves.

#### I. 4. Shift in position of terminal reference planes

Just as the phase angle of the reflection coefficient  $\Gamma$  defined by eq. (4) depends on the specific position along the lead, the phase angles of the elements of the scattering matrix  $S$  also vary with the choice of the origins of the respective  $z$ -axes. It is in this connection useful to study the transformation of  $S$  caused by a change of the origin of any  $z_n$ -axis. Referring to fig. 1, let the  $z'_n$ -axis be shifted over a distance  $l_n$  with respect to the  $z_n$ -axis away from the junction.

The appropriate phase shift is

$$\varphi_n = \beta_n l_n. \quad (10)$$

Denoting with a prime the quantities relating to the new origin, we have

$$a'_n = a_n e^{-i\varphi_n}, \quad b'_n = b_n e^{i\varphi_n}, \quad (11)$$

or in matrix notation

$$\mathbf{A}' = \Phi^{-1} \mathbf{A}, \quad \mathbf{B}' = \Phi \mathbf{B}. \quad (12)$$

$\Phi$  is a diagonal matrix with elements

$$\Phi_{nn} = e^{i\varphi_n}, \quad \Phi_{nm} = o(n \neq m). \quad (13)$$

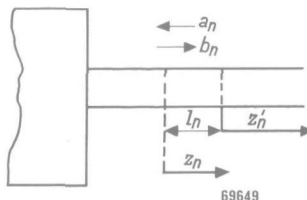


Fig. 1. An output lead of a waveguide junction showing the old and new  $z$ -axes.

Solving eqs (12) for  $\mathbf{A}$  and  $\mathbf{B}$  and inserting the result in eq. (9) we obtain

$$\Phi^{-1}\mathbf{B}' = \mathbf{S}\Phi\mathbf{A}', \quad (14)$$

or

$$\mathbf{B}' = \Phi\mathbf{S}\Phi\mathbf{A}'. \quad (15)$$

Hence it is seen that the scattering matrix  $\mathbf{S}'$ , related to the new origins, is connected to  $\mathbf{S}$  by the simple relation

$$\mathbf{S}' = \Phi\mathbf{S}\Phi. \quad (16)$$

### I. 5. Symmetry of the scattering matrix

The well-known principle of reciprocity in electrodynamics has a direct bearing on the scattering matrix. In fact it can be demonstrated that if reciprocity holds, as is guaranteed in our case by the conditions set out in Sec. 1, the scattering matrix is symmetrical.

The proof runs as follows. Let us consider the vector identity

$$\operatorname{div}(\mathbf{E}_1 \times \mathbf{H}_2 - \mathbf{E}_2 \times \mathbf{H}_1) = \mathbf{H}_2 \operatorname{curl} \mathbf{E}_1 - \mathbf{E}_1 \operatorname{curl} \mathbf{H}_2 - \mathbf{H}_1 \operatorname{curl} \mathbf{E}_2 + \mathbf{E}_2 \operatorname{curl} \mathbf{H}_1. \quad (17)$$

Here the subscripts 1 and 2 refer to two solutions of Maxwell's equations for the same junction and the same frequency but for different terminal conditions. Eliminating the curls with the aid of eqs (1) we find the right-hand side of eq. (17) to be identically zero. Hence

$$\operatorname{div}(\mathbf{E}_1 \times \mathbf{H}_2 - \mathbf{E}_2 \times \mathbf{H}_1) = 0. \quad (18)$$

Equation (18) is now integrated over the volume  $V$  of the junction and this integral is transformed into an integral over the surface  $F$  enclosing the junction and cutting the output leads perpendicularly to their respective  $z$ -axes. This gives

$$\int_V \operatorname{div}(\mathbf{E}_1 \times \mathbf{H}_2 - \mathbf{E}_2 \times \mathbf{H}_1) dV = \int_F (\mathbf{E}_1 \times \mathbf{H}_2 - \mathbf{E}_2 \times \mathbf{H}_1) d\mathbf{F} = 0. \quad (19)$$

$d\mathbf{F}$  is normal to the surface  $F$ . As the junction has been assumed to be perfectly shielded, the only contributions different from zero in eq. (19) come from those portions  $\Omega_n$  of the surface  $F$ , where it cuts the outputleads. Therefore

$$\int_F (\mathbf{E}_1 \times \mathbf{H}_2 - \mathbf{E}_2 \times \mathbf{H}_1) d\mathbf{F} = \sum_n \int_{\Omega_n} (\mathbf{E}_1 \times \mathbf{H}_2 - \mathbf{E}_2 \times \mathbf{H}_1) \mathbf{k}_n d\Omega_n = 0. \quad (20)$$

We now identify solution 1 with the case, that there is an incident wave in lead (1) only.

Solution 1: 
$$\begin{aligned} a_n &= 0 & n \neq 1, \\ b_n &= S_{n1} a_1 & . \end{aligned} \quad \} \quad (21)$$

In the same way

Solution 2: 
$$\begin{aligned} a_n &= 0 & n \neq 2, \\ b_n &= S_{n2} a_2 & . \end{aligned} \quad \} \quad (22)$$

Substituting eqs (21) and (22) together with eqs (2), (3) and (7) into eq. (20) we find that the only contributions come from leads (1) and (2). Evaluating these we obtain from lead (1)

$$(a_1 e^{-i\beta_1 z_1} + S_{11} a_1 e^{i\beta_1 z_1}) S_{12} a_2 e^{i\beta_1 z_1} + S_{12} a_2 e^{i\beta_1 z_1} (a_1 e^{-i\beta_1 z_1} - S_{11} a_1 e^{i\beta_1 z_1}) = 2 S_{12} a_1 a_2, \quad (23)$$

and from lead (2)

$$- S_{21} a_1 e^{i\beta_2 z_2} (a_2 e^{-i\beta_2 z_2} - S_{22} a_2 e^{i\beta_2 z_2}) - (a_2 e^{-i\beta_2 z_2} + S_{22} a_2 e^{i\beta_2 z_2}) S_{21} a_1 e^{i\beta_2 z_2} = -2 S_{21} a_1 a_2. \quad (24)$$

According to eq. (20) the quantities (23) and (24) add up to zero. Hence

$$S_{12} = S_{21}. \quad (25)$$

Now it is clear that only for the sake of clarity have we conducted the above argument specifically for leads (1) and (2). Nothing special has been assumed about them. Therefore eq. (25) can be generalized to

$$S_{nm} = S_{mn}, \quad (26)$$

or, in matrix notation,

$$\mathbf{S} = \tilde{\mathbf{S}}, \quad (27)$$

where  $\tilde{\mathbf{S}}$  represents the transpose of  $\mathbf{S}$ . This completes the proof that the scattering matrix is symmetrical. It is to be noted that the validity of this result is closely linked with the particular choice of the normalization condition, eq. (7).

## I. 6. Lossless junctions

If a junction is lossless, it follows from physical considerations that, once a stationary state has been attained ( $\omega$  real), the net power flow into the junction must be zero. It will be proved that as a consequence the scattering matrix of the junction must be unitary. We recall that a matrix is unitary if the product of its transpose with its complex conjugate yields the unit matrix.

Preceding this proof a general theorem will be derived that will be needed later on. Let us consider the identity

$$\operatorname{div} (\mathbf{E} \times \mathbf{H}^* + \mathbf{E}^* \times \mathbf{H}) = \mathbf{H}^* \operatorname{curl} \mathbf{E} - \mathbf{E} \operatorname{curl} \mathbf{H}^* + \mathbf{H} \operatorname{curl} \mathbf{E}^* - \mathbf{E}^* \operatorname{curl} \mathbf{H}. \quad (28)$$

The curls in eq. (28) can be eliminated with the aid of Maxwell's equations (1). In this connection complex values of  $\omega$  are allowed; on the other hand  $\epsilon$  and  $\mu$  are restricted to real values \*). The result is

$$\operatorname{div} (\mathbf{E} \times \mathbf{H}^* + \mathbf{E}^* \times \mathbf{H}) = i(\omega - \omega^*) \mu |H|^2 + \epsilon |E|^2 / 2\sigma |E|^2. \quad (29)$$

---

\*) This is only a formal restriction. Dielectric losses are already accounted for by  $\sigma$ . Losses of a magnetic nature could be easily included by adding a real term proportional to  $|H|^2$  on the right hand side of eq. (29).

This equation is integrated over the volume  $V$ ; the left hand side can be converted to a surface integral. Thus

$$\int_F (\mathbf{E} \times \mathbf{H}^* + \mathbf{E}^* \times \mathbf{H}) d\mathbf{F} = i(\omega - \omega^*) \int_V \{\mu|H|^2 + \varepsilon|E|^2\} dV - 2 \int_V \sigma|E|^2 dV. \quad (30)$$

It is to be noted that

$$\frac{1}{4} \int_V \{\mu|H|^2 + \varepsilon|E|^2\} dV = W \quad (31)$$

is the energy stored in the volume  $V$ . Further

$$\frac{1}{2} \int_V \sigma|E|^2 dV = D \quad (32)$$

is the power dissipated in the volume  $V$  and finally

$$\frac{1}{4} \int_F (\mathbf{E} \times \mathbf{H}^* + \mathbf{E}^* \times \mathbf{H}) d\mathbf{F} = P \quad (33)$$

represents the net power flowing through  $F$  out of  $V$ . Introducing the symbols  $W$ ,  $D$  and  $P$  in eq. (30) this takes the form

$$P = i(\omega - \omega^*) W - D. \quad (34)$$

If eq. (30) or eq. (34) is applied to a lossless junction for stationary states, the right hand side vanishes so that

$$P = \frac{1}{4} \int_F (\mathbf{E} \times \mathbf{H}^* + \mathbf{E}^* \times \mathbf{H}) d\mathbf{F} = 0. \quad (35)$$

The contributions of the various output leads to eq. (35) can be written explicitly. Thus

$$P = \frac{1}{2} \sum_n (b_n b_n^* - a_n a_n^*) = 0. \quad (36)$$

Introducing matrix notation we find that

$$\tilde{\mathbf{B}} \mathbf{B}^* - \tilde{\mathbf{A}} \mathbf{A}^* = 0. \quad (37)$$

Now  $\mathbf{B}$  can be eliminated by applying eq. (9), whence

$$\tilde{\mathbf{S}} \mathbf{A}^* \mathbf{A}^* - \tilde{\mathbf{A}} \mathbf{A}^* = 0, \quad (38)$$

or

$$\tilde{\mathbf{A}} (\tilde{\mathbf{S}} \mathbf{S}^* - \mathbf{I}) \mathbf{A}^* = 0. \quad (39)$$

Since eq. (30) is valid for all values of  $\mathbf{A}$ , it can be concluded that

$$\tilde{\mathbf{S}} \mathbf{S}^* = \mathbf{I}. \quad (40)$$

Thus the scattering matrix of a lossless junction is unitary.

## I. 7. Frequency dependence of a unitary scattering matrix

From a reasoning similar to that of the two previous sections a general expression for the frequency dependence of the scattering matrix of a

lossless junction can be derived. The result is equivalent to Foster's reactance theorem in network theory.

Consider the identity

$$\begin{aligned} \operatorname{div} (\mathbf{E}_1 \times \mathbf{H}_2^* + \mathbf{E}_2^* \times \mathbf{H}_1) &= \\ &= \mathbf{H}_2^* \operatorname{curl} \mathbf{E}_1 - \mathbf{E}_1 \operatorname{curl} \mathbf{H}_2^* + \mathbf{H}_1 \operatorname{curl} \mathbf{E}_2^* - \mathbf{E}_2^* \operatorname{curl} \mathbf{H}_1. \quad (41) \end{aligned}$$

Here the subscripts 1 and 2 refer to two solutions of Maxwell's equations for the same lossless structure but for different (real) frequencies. With the aid of eqs (1) the curls in the right hand side of eq. (41) can be eliminated:

$$\operatorname{div} (\mathbf{E}_1 \times \mathbf{H}_2^* + \mathbf{E}_2^* \times \mathbf{H}_1) = (\omega_1 - \omega_2) \langle \mu \mathbf{H}_1 \mathbf{H}_2^* + \epsilon \mathbf{E}_1 \mathbf{E}_2^* \rangle. \quad (42)$$

As before eq. (42) is integrated over the volume  $V$ , yielding

$$\int_F (\mathbf{E}_1 \times \mathbf{H}_2^* + \mathbf{E}_2^* \times \mathbf{H}_1) dF = i(\omega_1 - \omega_2) \int_V \langle \mu \mathbf{H}_1 \cdot \mathbf{H}_2^* + \epsilon \mathbf{E}_1 \cdot \mathbf{E}_2^* \rangle dV. \quad (43)$$

For  $\omega_1 = \omega_2$  eq. (43) is seen to become identical with eq. (35) as it should be.

Next we assume  $\omega_2$  to differ from  $\omega_1$  by an infinitesimal amount  $\delta\omega$ . The field quantities with index 2 then differ from  $\mathbf{E}_1$  and  $\mathbf{H}_1$  by small variations only, viz.

$$\begin{aligned} \delta \mathbf{E} &= \mathbf{E}_2 - \mathbf{E}_1, \\ \delta \mathbf{H} &= \mathbf{H}_2 - \mathbf{H}_1. \end{aligned} \quad (44)$$

Substituting eqs (44) in eq. (43) we obtain to the first order

$$\int_F (\mathbf{E} \times \delta \mathbf{H}^* + \delta \mathbf{E}^* \times \mathbf{H}) dF = -i\delta\omega \int_V \langle \mu |H|^2 + \epsilon |E|^2 \rangle dV = -4iW\delta\omega, \quad (45)$$

where the subscript 1 has been dropped as it is no longer needed.

On the left hand side of eq. (45) the contributions from the various terminal surfaces can be introduced explicitly. With the aid of eqs (2), (3) and (7) we find

$$\begin{aligned} \int_F (\mathbf{E} \times \delta \mathbf{H}^* + \delta \mathbf{E}^* \times \mathbf{H}) dF &= -\sum_n [(a_n e^{-i\beta_n z_n} + b_n e^{i\beta_n z_n}) (\delta a_n^* e^{i\beta_n z_n} - \\ &\quad - \delta b_n^* e^{-i\beta_n z_n}) + (\delta a_n^* e^{i\beta_n z_n} + \delta b_n^* e^{-i\beta_n z_n}) (a_n e^{-i\beta_n z_n} - b_n e^{i\beta_n z_n})] = \\ &= 2 \sum_n (b_n \delta b_n^* - a_n \delta a_n^*). \quad (46) \end{aligned}$$

Equation (46) can be written in matrix notation and combined with eq. (45) resulting in

$$\tilde{\mathbf{B}} \delta \mathbf{B}^* - \tilde{\mathbf{A}} \delta \mathbf{A}^* = -2iW\delta\omega. \quad (47)$$

Now  $\mathbf{B}$  can be eliminated according to

$$\tilde{\mathbf{B}} \delta \mathbf{B}^* = \tilde{\mathbf{S}} \mathbf{A} (\delta \mathbf{S}^* \mathbf{A}^* + \mathbf{S}^* \delta \mathbf{A}^*) = \tilde{\mathbf{A}} \tilde{\mathbf{S}} \delta \mathbf{S}^* \mathbf{A}^* + \tilde{\mathbf{A}} \delta \mathbf{A}^*. \quad (48)$$

Substitution of eq. (48) in eq. (47) gives

$$\tilde{\mathbf{A}}^* \tilde{\mathbf{S}} \delta \mathbf{S}^* \mathbf{A}^* = -2 i W \delta\omega. \quad (49)$$

Taking the complex conjugate of eq. (49) and putting

$$\frac{\delta \mathbf{S}}{\delta\omega} = \frac{d\mathbf{S}}{d\omega}, \quad (50)$$

we finally obtain the equation for the derivative of the scattering matrix of a lossless junction with respect to frequency, viz.

$$\tilde{\mathbf{A}}^* \tilde{\mathbf{S}}^* \frac{d\mathbf{S}}{d\omega} \mathbf{A} = 2 i W. \quad (51)$$

We shall now apply this general result to the special case of a single waveguide terminated by a lossless structure. The matrices in eq. (51) then reduce to scalars;  $\mathbf{S}$  degenerates to the reflection coefficient  $\Gamma(z=0)$ . Hence

$$a^* \Gamma^* \frac{d\Gamma}{d\omega} a = 2 i W. \quad (52)$$

As the termination is lossless, the “matrix”  $\Gamma$  is unitary or

$$\Gamma \Gamma^* = 1. \quad (53)$$

This equation is satisfied by putting

$$\Gamma = e^{i\varphi}, \quad (54)$$

where  $\varphi$  is restricted to real values. We further notice that the power incident on the junction  $P_i$  is given by

$$P_i = \frac{1}{2} a^* a. \quad (55)$$

If eqs (54) and (55) are substituted into eq. (52), the final result

$$\frac{d\varphi}{d\omega} = \frac{W}{P_i} \quad (56)$$

is obtained. This equation is important not so much for the quantitative information which it gives as for the fact that the right hand side is essentially positive. Thus

$$\frac{d\varphi}{d\omega} > 0, \quad (57)$$

or in words: for a lossless termination the phase angle of the reflection coefficient always increases with frequency.

## CHAPTER II. RESONATORS

In this chapter we shall be concerned with transducer theory for structures exhibiting resonance phenomena. As stated in the introduction, in writing the next pages we have been inspired by a little-known paper of Tomonaga<sup>3)</sup>. This paper contains much valuable material, but it has one serious shortcoming in that it deals with lossless structures only. Although this idealization is justified for many practical configurations, it forms especially for resonators a prohibitive restriction. We shall, accordingly, extend Tomonaga's theory so as to include the effect of losses.

### II. 1. Quality factor

We start by reviewing the essential property in which a resonator differs from other junctions. Let us assume that a certain amount of energy has been fed into a junction. If now the junction is left to itself and if it contains a resonating element, outgoing exponentially damped waves will appear in the output leads, which are for the moment assumed to be terminated by matched loads. In other words the amount of electromagnetic energy, stored inside the junction, is gradually decreasing because of the power loss through the various output leads and the dissipation inside the junction proper. It is this gradual exponential decrease of the stored energy (and at the same time of the amplitudes of the corresponding outgoing waves) which forms the characteristic feature of a resonator.

It is well known that microwave resonators have an infinite number of resonance frequencies. In the following we will develop the theory under the following restrictions. The angular frequency  $\omega$  shall lie close to one resonance frequency and be far removed from all others. This particular resonance frequency shall moreover be simple, i.e. there shall be only one mode of oscillation associated with it. Both conditions are fulfilled in many practically important cases. The theory, however, may readily be extended so as to include more general possibilities.

The theorem derived in Sec. I.6, eq. (34), furnishes quantitative information on the decrement of the oscillation in a resonator. We apply this equation

$$P = i(\omega_c - \omega_c^*) W - D, \quad (1)$$

to the case when no power is incident on the junction. Then  $P$  stands for the power leaving the junction through the various output leads,  $D$  is the power dissipated within the junction and  $W$  denotes the stored energy. The damped oscillation is described as an oscillation with a complex angular frequency  $\omega_c$ .

It will be remembered that the quality factor  $Q$  of a resonator can be defined as

$$Q = \frac{\omega_0 W}{D + P}, \quad (2)$$

where  $\omega_0$  is the real part of  $\omega_c$ .

Equation (2) can be rewritten as

$$\frac{1}{Q} = \frac{1}{\omega_0 W} \{D + \sum_n P_n\}, \quad (3)$$

or

$$\frac{1}{Q_L} = \frac{1}{Q_U} + \sum_n \frac{1}{Q_{E_n}}. \quad (4)$$

Apparently  $Q_L^{-1}$  is the sum of the contribution from internal losses  $D/\omega_0 W = Q_U^{-1}$  plus the contributions from each output lead individually  $P_n/\omega_0 W = Q_{E_n}^{-1}$ . Here a notation is employed which is customary in microwave work.  $Q_L$ , to be identified with  $Q$  in eq. (2), is called the loaded  $Q$  and represents the quality factor of the resonator loaded by all output leads. The partial  $Q$ 's introduced in eq. (4) are divided into the unloaded  $Q$ , denoted by  $Q_U$ , and various external  $Q$ 's, denoted by  $Q_{E_n}$ , each representing the loading effect of one output lead.

Attention should be drawn to the fact that in eq. (3) the terms  $D$  and  $P_n$  appear in a similar way. Whilst in eq. (I.30) their different origins are clearly indicated, in eq. (3) there is left only a formal difference in notation. The situation is, indeed, not altered if the term involving  $D$  is supposed to be due to an extra output lead, the junction itself being lossless. The advantage gained by this point of view is that we can start calculations with a unitary \*) scattering matrix for the idealized junction, introducing the internal losses only at a later stage. It should never be forgotten, however, that this is a purely formal way of approach and that, whilst  $N$  output leads of the junction are accessible for direct measurement, the fictitious lead numbered  $(N + 1)$  is not.

This procedure, viz. the concentration of the distributed losses within the junction into a fictitious extra output lead, is identical with the representation of the internal losses by a lumped resistance in equivalent circuit theory. Compared with the latter our point of view seems to be slightly superior in that no further assumption about the nature of the fictitious output lead is necessary whereas we must always assign a definite location to a lumped resistance.

\*) The scattering matrix of a lossless junction is unitary. This property is a direct result of the conservation of energy within the junction. The lemma therefore is true only for real frequencies as is also evident from the proof in Sec. I. 6.

The relation between the decrement of damped oscillations in a resonator and its  $Q$ -factor is obtained by combining eqs (1) and (2). Thus

$$i(\omega_c - \omega_c^*) = \frac{\omega_0}{Q}. \quad (5)$$

## II. 2. Fundamental considerations

Reverting now our attention to the scattering matrix we recall that its elements represent the ratio between amplitudes of outgoing and incident waves. In the preceding section we have discussed the state of a resonator with only outgoing waves in the output leads. A complex frequency  $\omega_c$  was used to describe these damped waves. Considering the elements of the scattering matrix as functions in the complex  $\omega$ -plane, it is clear that some, if not all, elements become infinite if the frequency approaches the value  $\omega_c$ . The most obvious possibility is that this singularity is a simple pole. Consequently we write tentatively

$$S_{nm} = \frac{p_{nm}}{\omega - \omega_c} + R_{nm}, \quad (6)$$

where  $p_{nm}$  and  $R_{nm}$  are independent of  $\omega$ . By the latter assumption we restrict the validity of eq. (6) a priori to that frequency range where the non-resonant frequency-dependence of the junction is completely obscured by the properties of the resonating element. Equation (6) therefore is at best valid in the neighbourhood of resonance.

With the aid of the following argument \*) it can be shown that eq. (6) is a plausible approximation. Suppose that along lead ( $m$ ) a pulse of infinitesimal duration is fed into the resonator. This incoming signal can be represented by <sup>5)</sup>

$$a_m = \lim_{\tau \rightarrow 0} \frac{1}{2\pi} \int_{-\infty}^{+\infty} \frac{\sin (\omega\tau/2)}{\omega\tau/2} e^{-i\omega t} d\omega. \quad (7)$$

The outgoing waves  $b_n$ , caused by  $a_m$ , are obtained by multiplying the integrand in eq. (7) by the appropriate element  $S_{nm}$ . Inserting eq. (6) we have

$$\begin{aligned} b_n = p_{nm} \lim_{\tau \rightarrow 0} \frac{1}{2\pi} \int_{-\infty}^{+\infty} & \frac{\sin (\omega\tau/2)}{\omega\tau/2} \frac{e^{-i\omega t}}{\omega - \omega_c} d\omega + \\ & + R_{nm} \lim_{\tau \rightarrow 0} \frac{1}{2\pi} \int_{-\infty}^{+\infty} \frac{\sin (\omega\tau/2)}{\omega\tau/2} e^{-i\omega t} d\omega. \end{aligned} \quad (8)$$

\*) This proof was suggested to the author by Prof. Dr H. B. G. Casimir, Director Philips Research Laboratories.

The first term on the right-hand side of eq. (8) can be evaluated by closing the path of integration by a semicircle of infinite radius in the negative imaginary half plane. Taking the limit  $\tau \rightarrow 0$  and applying the theorem of residues we find

$$b_n = -i p_{nm} e^{-i\omega c t} + R_{nm} \lim_{\tau \rightarrow 0} \frac{1}{2\pi} \int_{-\infty}^{+\infty} \frac{\sin(\omega\tau/2)}{\omega\tau/2} e^{-i\omega t} d\omega. \quad (9)$$

The last term in eq. (9) represents an outgoing pulse of which the amplitude is determined by the non-resonant properties of the junction. The first term on the right in eq. (9) indicates, that part of the energy contained in the incident pulse is temporarily stored within the junction and leaks away only gradually through the output leads. This behaviour agrees exactly with the views developed in Sec. I on resonators. The assumption that  $S_{nm}$  has a simple pole for  $\omega = \omega_c$  is thus seen to be well-founded.

From the preceding argument another important conclusion can be drawn. It follows from eq. (9) that the amplitudes of the outgoing damped waves, caused by the pulse incident in lead ( $m$ ), are proportional to the coefficients  $p_{nm}$ . Nothing special has been assumed about lead ( $m$ ); it is clearly immaterial through which lead the energy, giving rise to the outgoing damped waves, is brought into the resonator. Therefore the ratios of the coefficients  $p_{nm}$  ( $m$  fixed) should be independent of  $m$ . This fact together with the symmetry condition for the scattering matrix, which property is not restricted to real values of  $\omega$  (cf. Sec. I, 5), requires, that all  $p_{nm}$  have the form

$$p_{n\bar{m}} = \pi_n \pi_m. \quad (10)$$

### II. 3. Resonators with one output lead

Instead of deriving the general theory for resonant junctions with any number of output leads we shall conduct the discussion along simpler lines by working out some practically important examples. Occasionally the obvious extensions to the more general case will be pointed out.

As a first example we shall analyse the behaviour of a resonator with one output lead; the coupling between resonator and output lead is supposed to be lossless. According to the argument developed at the end of Sec. I the situation can be schematically represented by fig. 2.1. The actual internal losses are accounted for by the matched termination in lead (2), while the resonant junction between the leads is lossless.

The scattering matrix for this structure is, according to eqs (6) and (10),

$$S = \begin{pmatrix} S_{11} & S_{12} \\ S_{12} & S_{22} \end{pmatrix} = \begin{pmatrix} \frac{\pi_1^2}{\omega - \omega_c} + R_{11} & \frac{\pi_1 \pi_2}{\omega - \omega_c} + R_{12} \\ \frac{\pi_1 \pi_2}{\omega - \omega_c} + R_{12} & \frac{\pi_2^2}{\omega - \omega_c} + R_{22} \end{pmatrix}. \quad (11)$$

The symmetry condition for  $S$  has been used in eq. (11). The unitary condition requires

$$\begin{aligned} |S_{11}|^2 + |S_{12}|^2 &= |S_{12}|^2 + |S_{22}|^2 = 1, \\ S_{11}S_{12}^* + S_{12}S_{22}^* &= 0. \end{aligned} \quad (12)$$

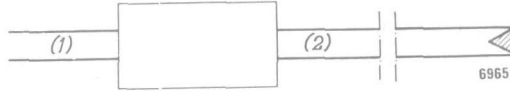


Fig. 2.1. Schematic representation of a resonator with one output lead. The matched termination in the (fictitious) lead (2) accounts for the internal losses.

These conditions must be fulfilled for all real values of  $\omega$ . If eq. (11) is substituted in eqs (12), terms appear in  $(\omega - \omega_c)^{-1}$ ,  $(\omega - \omega_c^*)^{-1}$  and  $(\omega - \omega_c)^{-1}$ ,  $(\omega - \omega_c^*)^{-1}$ . The latter can be expanded in partial fractions, so that the resulting equations take the form

$$\frac{A}{\omega - \omega_c} + \frac{B}{\omega - \omega_c^*} + C = 0, \quad (13)$$

where  $A$ ,  $B$  and  $C$  are not dependent on  $\omega$ . If an equation like eq. (13) is to hold for all  $\omega$ , then  $A = 0$ ,  $B = 0$  and  $C = 0$  (note that  $\omega_c$  is not real). The knowledge that the terms  $C$  are zero immediately leads to the result that the matrix

$$\mathbf{R} = \begin{pmatrix} R_{11} & R_{12} \\ R_{12} & R_{22} \end{pmatrix} \quad (14)$$

is unitary. Actually this fact could have been deduced directly from eq. (11), as  $\mathbf{R}$  represents the behaviour of the lossless junction far off resonance.

The remaining equations are obtained from the coefficients of  $(\omega - \omega_c)^{-1}$  and  $(\omega - \omega_c^*)^{-1}$  in eqs (12) and are

$$\pi_1^* \left| \pi_1 \right|^2 + \left| \pi_2 \right|^2 + (R_{11}^* \pi_1 + R_{12}^* \pi_2) (\omega_c - \omega_c^*) = 0, \quad (15)$$

$$\pi_2^* \left| \pi_1 \right|^2 + \left| \pi_2 \right|^2 + (R_{12}^* \pi_1 + R_{22}^* \pi_2) (\omega_c - \omega_c^*) = 0. \quad (16)$$

Equations (15) and (16) are identical with the matrix equation

$$(\tilde{\Pi} \Pi^*) \Pi^* + (\omega_c - \omega_c^*) \mathbf{R}^* \Pi = 0, \quad (17)$$

where the column matrix  $\Pi$  is given by

$$\Pi = \begin{pmatrix} \pi_1 \\ \pi_2 \end{pmatrix}. \quad (18)$$

From eq. (17)  $\mathbf{R}$  can be eliminated. As  $\mathbf{R}$  is unitary, multiplication of eq. (17) by  $\mathbf{R}$  and a subsequent change to the complex conjugate yields

$$(\tilde{\Pi}\Pi^*)\mathbf{R}^*\Pi - (\omega_c - \omega_c^*)\Pi^* = 0. \quad (19)$$

By combination of eqs (17) and (19) we obtain

$$(\tilde{\Pi}\Pi^*)^2 = -(\omega_c - \omega_c^*)^2. \quad (20)$$

As  $\omega_c$  is the frequency of a damped oscillation, it has a negative imaginary part; hence the positive root of eq. (20) is the correct one, so that

$$\tilde{\Pi}\Pi^* = |\pi_1|^2 + |\pi_2|^2 = i(\omega_c - \omega_c^*). \quad (21)$$

Equation (5) enables us to introduce the experimentally important parameters  $\omega_0$  and  $Q_L$ :

$$|\pi_1|^2 + |\pi_2|^2 = \frac{\omega_0}{Q_L}. \quad (22)$$

In Sec. 1 we have seen, that the internal losses and the loading due to the output lead contribute separately to  $Q_L^{-1}$ . Equation (4) adapted to the present problem can be written as

$$\frac{1}{Q_L} = \frac{1}{Q_E} + \frac{1}{Q_U} = \frac{1}{Q_1} + \frac{1}{Q_2}. \quad (23)$$

Comparison with eq. (22), where  $Q_L^{-1}$  also appears as a sum of contributions from each output lead individually, compels us to conclude that

$$|\pi_1|^2 = \frac{\omega_0}{Q_1} = \frac{\omega_0}{Q_E}, \quad |\pi_2|^2 = \frac{\omega_0}{Q_2} = \frac{\omega_0}{Q_U}. \quad (24)$$

The relation between  $\Pi$  and  $\mathbf{R}$  can be derived by insertion of eq. (21) into eq. (17). The complex conjugate of the result is

$$\mathbf{R}\Pi^* = i\Pi. \quad (25)$$

As was pointed out before  $\mathbf{R}$  describes the off-resonance behaviour of the resonator. The condition that the coupling between resonator and output lead is lossless implies total reflection far off resonance. Hence the off-diagonal elements of  $\mathbf{R}$  must vanish and eq. (25) results in separate equations for  $\pi_1$  and  $\pi_2$ . Anticipating the needs for the next section, however, we shall derive the consequences of eq. (25) without imposing any restriction on  $\mathbf{R}$ .

But for the asterisk eq. (25) would have been an eigenvalue equation for  $\mathbf{R}$ . It can be brought into this form by splitting up  $\Pi$  into modulus and argument, viz.

$$\Pi = \begin{pmatrix} \pi_1 \\ \pi_2 \end{pmatrix} = \begin{pmatrix} e^{i\varphi_1} & 0 \\ 0 & e^{i\varphi_2} \end{pmatrix} \begin{pmatrix} |\pi_1| \\ |\pi_2| \end{pmatrix} = \Phi |\Pi|. \quad (26)$$

Substitution of eq. (26) in eq. (25) yields

$$\mathbf{R}\Phi^*|\Pi| = i\Phi|\Pi|. \quad (27)$$

Premultiplication of both sides of eq. (27) by  $\Phi^{-1} = \Phi^*$  gives

$$\Phi^{-1}\mathbf{R}\Phi^{-1}|\Pi| \equiv \mathbf{R}'|\Pi| = i|\Pi|. \quad (28)$$

The matrix  $\mathbf{R}'$ , introduced in eq. (28), is derived from  $\mathbf{R}$  by a simple shift of the reference planes in the output leads, as follows from Sec. I.4. The shift is chosen so as to make the quantities  $\pi'_n = |\pi_n|$  real.

Equation (28) is an eigenvalue equation. The limitation it imposes on  $\mathbf{R}'$  consists in the prescription of an eigenvalue  $i$  with a corresponding eigenvector proportional to  $|\Pi|$ . The second eigenvalue of  $\mathbf{R}'$  is a priori unknown but its magnitude should equal 1, because  $\mathbf{R}'$ , like  $\mathbf{R}$ , is unitary. The second eigenvector is fixed by the condition that it should be real and orthogonal to  $|\Pi|$ . We are now able to form  $\mathbf{R}'$  from its eigenvalues and eigenvectors. The latter are normalized to unity. Let the second eigenvalue be  $i e^{2i\eta}$ ,  $\eta$  being real but otherwise unknown. In this way we obtain

$$\mathbf{R}' = \mathbf{M} \begin{pmatrix} i & 0 \\ 0 & i e^{2i\eta} \end{pmatrix} \mathbf{M}, \quad (29)$$

with

$$\mathbf{M} = \mathbf{M}^{-1} = \begin{pmatrix} \sqrt{\frac{Q_L}{Q_1}} & \sqrt{\frac{Q_L}{Q_2}} \\ \sqrt{\frac{Q_L}{Q_2}} & -\sqrt{\frac{Q_L}{Q_1}} \end{pmatrix}. \quad (30)$$

Reference to eq. (24) shows that the first column of the orthogonal matrix  $\mathbf{M}$  is, indeed, proportional to  $|\Pi|$ .

Evaluating eq. (29) we find for  $\mathbf{R}'$  the general expression

$$\mathbf{R}' = \begin{pmatrix} i - 2 \frac{Q_L}{Q_2} \sin\eta e^{i\eta} & 2 \frac{Q_L}{\sqrt{Q_1 Q_2}} \sin\eta e^{i\eta} \\ 2 \frac{Q_L}{\sqrt{Q_1 Q_2}} \sin\eta e^{i\eta} & i - 2 \frac{Q_L}{Q_1} \sin\eta e^{i\eta} \end{pmatrix}. \quad (31)$$

In the special case that the off-diagonal elements of  $\mathbf{R}'$  vanish, eq. (31) reduces to the almost trivial form

$$\mathbf{R}' = \begin{pmatrix} i & 0 \\ 0 & i \end{pmatrix}. \quad (32)$$

The reflection coefficient  $\Gamma'$  seen in output lead (1), if output lead (2) is terminated by a matched load, becomes identical with  $S_{11}$ . Insertion of eqs (24) and (32) into eq. (11) yields

$$\Gamma' = S'_{11} = \frac{\omega_0}{Q_E(\omega - \omega_c)} + i. \quad (33)$$

Equation (33) represents the reflection coefficient in the output lead of the resonator at the particular reference plane fixed by eq. (28).

It is useful to eliminate  $\omega_c$  from eq. (33) and to replace it by quantities better suited to measurement. To this purpose put, as is customary,

$$\omega - \omega_0 = \Delta\omega. \quad (34)$$

Then

$$\omega - \omega_c = \Delta\omega - \frac{1}{2}(\omega_c - \omega_c^*). \quad (35)$$

With the aid of eqs (5) and (35) eq. (33) can be brought into its final form

$$\Gamma' = -i \frac{2Q_L}{Q_E(1 - 2i Q_L \Delta\omega/\omega_0)} + i. \quad (36)$$

The locus of  $\Gamma'$  in the complex plane as a function of frequency is a circle of radius  $Q_L/Q_E$  tangent to the unit circle at the point  $i$ , as is illustrated in fig. 2.2. It should be remembered that eq. (36) is valid for one particular reference plane. A shift of the reference plane simply corresponds to a rotation of the locus around the origin.

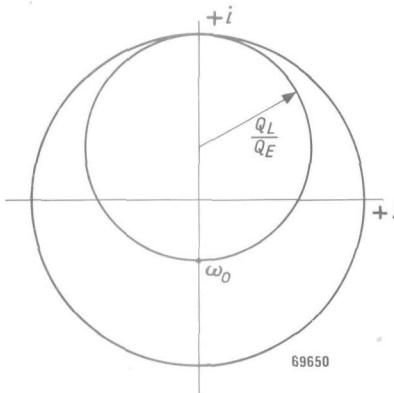


Fig. 2.2. Locus of the reflection coefficient in a waveguide terminated by a resonator.

## II. 4. Resonators with two output leads

As a second example of the use of a scattering matrix, the elements of which can be represented by eq. (6), we shall discuss the case of a resonator with two output leads attached to it. In the diagram of fig. 2.3 the output leads are designated (1) and (2). Output lead (3) accounts for the internal losses of the resonator, so that the scattering matrix pertinent to the rectangle containing the resonator is unitary. Both the coupling between the resonator and its output leads and the direct (i.e. off-resonance) coupling between leads (1) and (2) are assumed to be lossless. As the matched load in lead (3) represents formally the losses within the resonator, no direct coupling will occur between lead (3) and the other two output leads. The off-resonance matrix  $\mathbf{R}$  will therefore be

$$\mathbf{R} = \begin{pmatrix} R_{11} & R_{12} & 0 \\ R_{12} & R_{22} & 0 \\ 0 & 0 & R_{33} \end{pmatrix}. \quad (37)$$

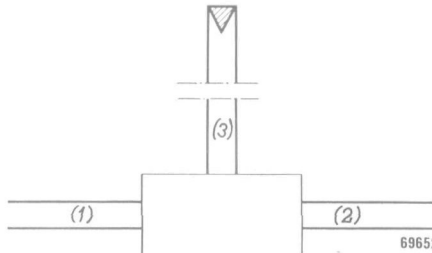


Fig. 2.3. Schematical representation of a resonator with two output leads. The matched termination in the (fictitious) lead (3) accounts for the internal losses.

For the present problem we require an obvious extension of some results of the preceding section. The proof, if needed, can be given in exact analogy to the treatment in Sec. 3. In fact, all matrix equations derived there are generally valid, irrespective of the order of the matrices, i.e. the number of output leads.

The matrix  $\mathbf{R}$  is unitary. As a consequence the submatrix

$$\begin{pmatrix} R_{11} & R_{12} \\ R_{12} & R_{22} \end{pmatrix} \quad (38)$$

is also unitary.

The equations equivalent to eqs (23) and (24) are

$$\frac{1}{Q_L} = \frac{1}{Q_1} + \frac{1}{Q_2} + \frac{1}{Q_3}, \quad (39)$$

and

$$|\pi_1|^2 = \frac{\omega_0}{Q_1}, \quad |\pi_2|^2 = \frac{\omega_0}{Q_2}, \quad |\pi_3|^2 = \frac{\omega_0}{Q_3}. \quad (40)$$

To analyse the relation between  $\mathbf{R}$  and  $\Pi$  it is useful to define the reference planes again in such a way that the elements of  $\Pi$  become real and eq. (28) applies. Because of eq. (37), eq. (28) falls apart in separate equations for  $R'_{33}$  and the submatrix (38); the latter equation is

$$\begin{pmatrix} R'_{11} & R'_{12} \\ R'_{12} & R'_{22} \end{pmatrix} \begin{pmatrix} |\pi_1| \\ |\pi_2| \end{pmatrix} = i \begin{pmatrix} |\pi_1| \\ |\pi_2| \end{pmatrix}. \quad (41)$$

The conclusions to be drawn from this equation are almost literally the same as eqs (29) and (30) of the previous section; the only difference lies in the normalization of the modal matrix  $\mathbf{M}$ . Thus

$$\begin{pmatrix} R'_{11} & R'_{12} \\ R'_{12} & R'_{22} \end{pmatrix} = \mathbf{M} \begin{pmatrix} i & 0 \\ 0 & ie^{2i\eta} \end{pmatrix} \mathbf{M}, \quad (42)$$

where

$$\mathbf{M} = \mathbf{M}^{-1} = \begin{pmatrix} \sqrt{\frac{Q_E}{Q_1}} & \sqrt{\frac{Q_E}{Q_2}} \\ \sqrt{\frac{Q_E}{Q_2}} & -\sqrt{\frac{Q_E}{Q_1}} \end{pmatrix}. \quad (43)$$

Here we have introduced the symbol  $Q_E$  to represent the total external loading of the resonator, which is given by

$$\frac{1}{Q_E} = \frac{1}{Q_1} + \frac{1}{Q_2}. \quad (44)$$

Evaluating eq. (42) we find

$$\begin{pmatrix} R'_{11} & R'_{12} \\ R'_{12} & R'_{22} \end{pmatrix} = \begin{pmatrix} i - 2 \frac{Q_E}{Q_2} \sin \eta e^{i\eta} & 2 \frac{Q_E}{\sqrt{Q_1 Q_2}} \sin \eta e^{i\eta} \\ 2 \frac{Q_E}{\sqrt{Q_1 Q_2}} \sin \eta e^{i\eta} & i - 2 \frac{Q_E}{Q_1} \sin \eta e^{i\eta} \end{pmatrix}. \quad (45)$$

Output lead (3) is now assumed to be terminated by a matched load. The scattering matrix for the resonant junction between leads (1) and (2) is obtained by omitting the third row and column from the matrix pertaining to the lossless junction discussed up till now. By eqs (6), (10) and (40) we have

$$S' = \begin{pmatrix} \frac{\omega_0}{Q_1(\omega - \omega_c)} + R'_{11} & \frac{\omega_0}{\sqrt{Q_1 Q_2}(\omega - \omega_c)} + R'_{12} \\ \frac{\omega_0}{\sqrt{Q_1 Q_2}(\omega - \omega_c)} + R'_{12} & \frac{\omega_0}{Q_2(\omega - \omega_c)} + R'_{22} \end{pmatrix}. \quad (46)$$

It is possible to eliminate  $\omega_c$  again by the introduction of  $\Delta\omega = \omega - \omega_0$ . If further eq. (45) is substituted in eq. (46), the final expression becomes

$$S' = \begin{pmatrix} -i \frac{2Q_L}{Q_1(1 - 2iQ_L \Delta\omega/\omega_0)} + i - 2 \frac{Q_E}{Q_2} \sin\eta e^{i\eta} - \\ -i \frac{2Q_L}{\sqrt{Q_1 Q_2}(1 - 2iQ_L \Delta\omega/\omega_0)} + 2 \frac{Q_E}{\sqrt{Q_1 Q_2}} \sin\eta e^{i\eta} - \\ -i \frac{2Q_L}{\sqrt{Q_1 Q_2}(1 - 2iQ_L \Delta\omega/\omega_0)} + 2 \frac{Q_E}{\sqrt{Q_1 Q_2}} \sin\eta e^{i\eta} \\ -i \frac{2Q_L}{Q_2(1 - 2iQ_L \Delta\omega/\omega_0)} + i - 2 \frac{Q_E}{Q_1} \sin\eta e^{i\eta} \end{pmatrix}. \quad (47)$$

An instrument to which eq. (47) is applicable is the iris-coupled reaction wavemeter shown in fig. 2.4. It is not an example of eq. (47) in its most general form, as the symmetrical location of the two output leads obviously requires

$$Q_1 = Q_2. \quad (48)$$

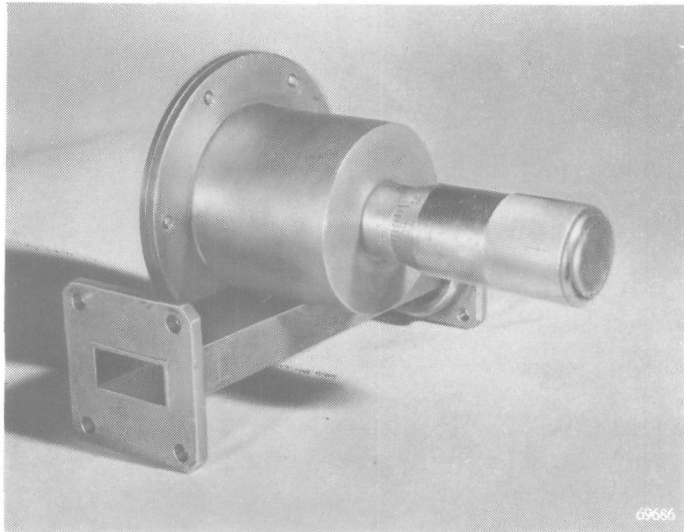


Fig. 2.4. Reaction wavemeter.

After insertion of this condition into eq. (44), eq. (47) can be simplified to

$$S' = \begin{pmatrix} -i \frac{Q_L}{Q_E(1-2iQ_L\Delta\omega/\omega_0)} + i - \sin\eta e^{i\eta} & -i \frac{Q_L}{Q_E(1-2iQ_L\Delta\omega/\omega_0)} + \sin\eta e^{i\eta} \\ -i \frac{Q_L}{Q_E(1-2iQ_L\Delta\omega/\omega_0)} + \sin\eta e^{i\eta} & -i \frac{Q_L}{Q_E(1-2iQ_L\Delta\omega/\omega_0)} + i - \sin\eta e^{i\eta} \end{pmatrix}. \quad (49)$$

The transmission coefficient from lead (1) to lead (2) or vice versa is given by the off-diagonal elements in eq. (49). As a function of frequency it is represented in the complex plane by a circle of radius  $Q_L/Q_1 = Q_L/2Q_E$ . The position of this circle is determined by the value of  $\eta$ ; its centre in particular lies on a circle, which we shall call  $\eta$ -circle, of radius  $\frac{1}{2}$  centred on the imaginary axis at the point  $(Q_L/2Q_3)i = (Q_L/2Q_U)i$ , as is illustrated in fig. 2.5.

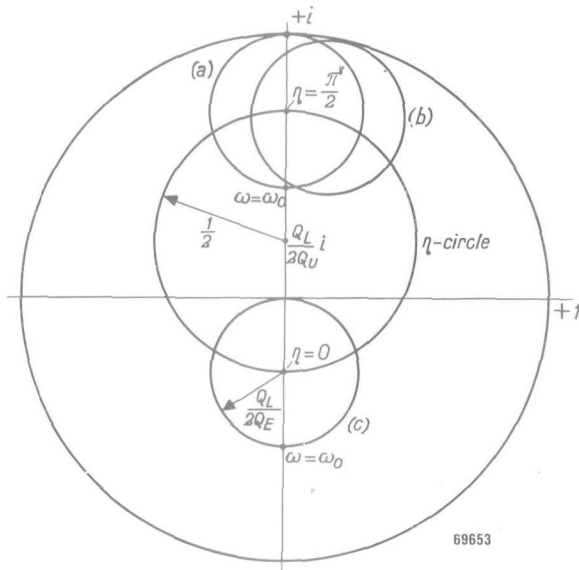


Fig. 2.5. Transmission-coefficient diagram for a resonator with two symmetrical output leads.

For the ideal reaction wavemeter, in which the off-resonance reflection caused by the coupling window is suitably compensated, the appropriate value of  $\eta$  is  $\frac{1}{2}\pi$ . Its transmission coefficient is represented in fig. 2.5 by the circle (a).

The behaviour of a non-compensated reaction wavemeter is illustrated by the circle (b) the centre of which lies on the  $\eta$ -circle slightly off the imaginary axis.

The circle (c), for which  $\eta = 0$ , shows that eq. (49) also applies to wavemeters of the transmission type. It represents the transmission coefficient

through a resonator with two symmetrically located output leads between which no direct coupling exists.

Dropping the restriction imposed by eq. (48) for symmetrical output leads we can deduce from eq. (47), for the case  $\eta = 0$ , that the condition for a match in output lead (1) at the resonance frequency is

$$\frac{2Q_L}{Q_1} = 1, \quad (50)$$

or

$$\frac{Q_U}{Q_1} = \frac{Q_U}{Q_2} + 1. \quad (51)$$

As a final remark it should be pointed out that the rather artificial difference between series and parallel resonant circuits, usual in equivalent-circuit theory, is completely avoided here.

## II. 5. Losses in the output circuit

The theory developed in the preceding section can be made, by a slight modification, to describe the behaviour of a resonator coupled to an ideal waveguide through a circuit of which the losses cannot be neglected. To this purpose the schematical representation of fig. 2.3. is redrawn in fig. 2.6. The output circuit is idealized to a frequency-independent T-junction. Its losses are lumped in the matched load of lead (2), while lead (3) is again included to account for the internal losses of the resonator. The configuration depicted in fig. 2.6 is a useful approximation for the analysis of a "cold" oscillator tube<sup>6), 7)</sup>. Formally figs 2.3 and 2.6 are identical, so that eq. (47) is equally valid in the two cases.

If both leads (2) and (3) are terminated by a matched load, the reflection coefficient  $\Gamma'$  in lead (1) is given by  $S_{11}$ . Hence, from eq. (47)

$$\Gamma' = -i \frac{2Q_L}{Q_1(1 - 2iQ_L \Delta\omega/\omega_0)} + i - 2 \frac{Q_E}{Q_2} \sin\eta e^{i\eta}. \quad (52)$$

The locus of  $\Gamma'$  in the complex plane is commonly called the  $Q$ -circle.

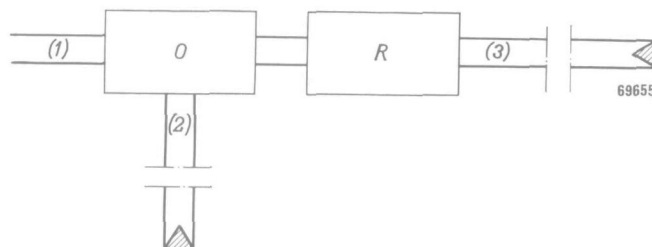


Fig. 2.6. Schematic representation of a resonator  $R$  with output circuit  $O$ .

Once this circle has been obtained by experiment, all parameters of the resonator can be derived from it as follows:

From the relation between  $\omega$  and  $\Gamma'$  on the circle  $Q_L$  can be determined. From the radius of the circle, which equals  $Q_L/Q_1$ ,  $Q_1$  is then calculated. It is seen from eq. (52) that the position of the centre of the  $Q$ -circle is determined by  $\eta$  and  $Q_2$ . For  $\eta = 0$  the  $Q$ -circle is tangent with its off-resonance point to the unit circle at the point  $i$ ; its centre lies for other values of  $\eta$  on the  $\eta$ -circle, centred on the imaginary axis, with radius  $Q_E/Q_2 = Q_1/(Q_1 + Q_2)$ . In fig. 2.7 it is shown how the  $\eta$ -circle can be derived from the  $Q$ -circle by a geometrical construction. As a first step the off-resonance point  $P$  must be located <sup>7)</sup>, which can be done by extrapolation only, as our fundamental assumptions in Sec. 2 restrict the validity of eq. (52) to the neighbourhood of resonance. The diameter of the  $Q$ -circle through  $P$  is drawn and parallel to it the diameter of the unit circle. The latter is to be identified with the imaginary axis; it should be realized that the reference plane for which eq. (52) applies is not known beforehand. The construction of the  $\eta$ -circle is now a simple matter, because it is known that (i) its centre lies on the imaginary axis, (ii) the centre of the  $Q$ -circle falls on it and (iii) it cuts the imaginary axis at a distance  $(Q_1 - Q_L)/Q_1$  from the origin. The geometrical consequences are illustrated in fig. 2.7. After the  $\eta$ -circle has been constructed,  $Q_2$  can be calculated from its radius. Finally  $Q_3 = Q_U$  can be found with the aid of eq. (39) from the known values of  $Q_L$ ,  $Q_1$  and  $Q_2$ .

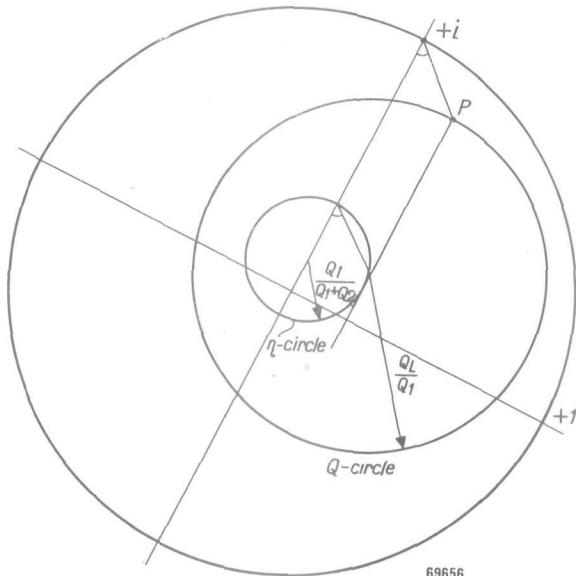


Fig. 2.7. The  $Q$ -circle and the  $\eta$ -circle.

### CHAPTER III. SYMMETRY ANALYSIS OF WAVEGUIDE JUNCTIONS

If a waveguide junction exhibits a certain degree of symmetry, the number of constants needed to describe its behaviour as a transducer is less than for the general non-symmetrical junction with the same number of output leads.

A method to perform this reduction of constants has first been given, for lossless structures, by Dicke<sup>1)</sup>. The scattering matrix of a lossless junction is unitary and can therefore always be brought into diagonal form by a suitable unitary similarity transformation. Dicke's method, accordingly, is one suitable to eigenvalue problems; he developed it largely by treating a number of specific examples.

In order to include dissipative structures, Kerns<sup>8)</sup> has lately put the theory on a more rigorous mathematical basis by extensive use of concepts derived from group theory. It is hardly necessary to point out that the methods used are for a large part identical with those developed for the analysis of symmetry problems in molecular physics<sup>9)</sup> and quantum mechanics<sup>10), 11)</sup>.

In this chapter we shall give an outline of Kerns' theory in conjunction with some aspects elaborated by Dicke. It is supposed that the reader is acquainted with the fundamental results of the theory of finite groups.

#### III. 1. Representation of a symmetry group

From the vector notation of Maxwell's equations (I. 1) it is clear that their validity is not restricted to a particular choice of coordinate system. If a new coordinate system is introduced by a real linear transformation from the original system and the field components are transformed accordingly, the latter will again satisfy Maxwell's equations. Mathematically we can say that Maxwell's equations are invariant with respect to the real linear group. A particular subgroup of this linear group is the three-dimensional rotation reflection group, which in its turn comprises the point-symmetry groups (also called the crystallographic groups).

The invariance of Maxwell's equations, though important, is in itself not very helpful. A new situation arises, however, if in a specific problem there can be found a transformation subject to which the boundary conditions also are invariant. Such a transformation is termed a covering operation for the structure under consideration. Because we deal only with structures of finite size, a translation cannot be a covering operation. The only possibilities left are reflections in a plane or a point and rotations about an axis. All possible covering operations of a structure, including the identity operator, constitute the symmetry group of the structure.

Let us consider now the electromagnetic field inside a waveguide junction. A covering operation will change the spatial position of the junction and the field, without altering their relative position. But as the junction remains by definition invariant under the operation, we may just as well assume the junction to be fixed in space, whilst the operation affects only the field within it.

In the previous chapters we have discussed, how the electromagnetic behaviour of a junction can be described by the amplitudes of waves in the output leads. Once the amplitudes of the incoming waves, represented by the column matrix  $A$ , are prescribed, the amplitudes  $B$  of the emergent waves are determined by the properties of the junction as expressed in terms of the scattering matrix. In Chap. I it has been explained, that the elements  $a_n$  and  $b_n$  of  $A$  and  $B$  respectively are to be regarded as coefficients for the transverse electric field  $E_{tn}$  in the various output leads of the junction. In other words we may state, that the fields  $E_{tn}$  constitute the coordinate system or basis for the description of the electromagnetic field;  $A$  comprises the coordinates of a possible incident electromagnetic field relative to this coordinate system and can as such be regarded as a vector.

If a covering operation  $P$  of the symmetry group of the structure is applied to  $A$ , we obtain another possible field  $PA$ . The coefficient  $a_n$ , describing before the operation the field in lead  $(n)$ , will after the operation pertain to the field in lead  $(m)$ . The normalizing condition, eq. (I. 7), requires, that the basis fields  $E_{tn}$  and  $E_{tm}$  at corresponding points for all leads  $(n)$  and  $(m)$  respectively which interchange under the covering operation, are connected by

$$|E_{tn}|^2 = |E_{tm}|^2. \quad (1)$$

It should be noted that the one-mode assumption, condition (v), Sec. I.1, is essential here. The origin of the time scale can always be chosen so that  $E_{tn}$  is real for all  $n$ . Then there are only two possible solutions of eq. (1), viz.

$$E_{tn} = \pm E_{tm}. \quad (2)$$

It follows from eq. (2), that the matrix  $D(P)$ , which expresses the vector  $PA$  in terms of  $A$ , consists only of elements 0, +1 and -1. In each row and column there is only one non-zero element. The matrix  $D(P)$  is therefore real and orthogonal.

For all operators  $P$  of the symmetry group the corresponding matrices  $D(P)$  can be formed. These matrices then constitute a representation of the group. The basis for this representation consists of the transverse electric fields in the output leads. It is evident that the dimension of the representation equals the number of output leads of the junction.

### III. 2. Relation between the symmetry of a junction and its scattering matrix

As our aim is the simplification of the scattering matrix of a junction, it is well to consider the connection between this quantity and the representation of the symmetry group.

Let  $\mathbf{A}$  and  $\mathbf{B}$  specify a possible solution of Maxwell's equations for the junction; then

$$\mathbf{B} = \mathbf{S}\mathbf{A}. \quad (3)$$

By definition the fields

$$\mathbf{A}' = \mathbf{D}(P)\mathbf{A}, \quad \mathbf{B}' = \mathbf{D}(P)\mathbf{B}, \quad (4)$$

obtained by a covering operation from  $\mathbf{A}$  and  $\mathbf{B}$ , constitute also a possible solution of Maxwell's equations. Hence

$$\mathbf{B}' = \mathbf{S}\mathbf{A}'. \quad (5)$$

Inserting eq. (4) in eq. (3) we have

$$\mathbf{D}(P)\mathbf{B} = \mathbf{S}\mathbf{D}(P)\mathbf{A}, \quad (6)$$

or by virtue of eq. (3)

$$\mathbf{D}(P)\mathbf{S}\mathbf{A} = \mathbf{S}\mathbf{D}(P)\mathbf{A}. \quad (7)$$

Equation (7) is valid for any  $\mathbf{A}$ , so that for any  $P$

$$\mathbf{D}(P)\mathbf{S} = \mathbf{S}\mathbf{D}(P). \quad (8)$$

Equation (8) tells us that the scattering matrix commutes with all matrices  $\mathbf{D}(P)$  of the representation of the symmetry group. This relation is the key to the solution of our problem.

The choice of the transverse electric fields in the output leads as a basis follows in a natural way from the physical properties of the structure and is in this respect the simplest possible. However, this does not imply that it is, mathematically, the most logical choice for the analysis of eq. (8) and in general it will not be so. If then we want to analyse the influence of the symmetry properties of a junction on its electromagnetic behaviour, it will be wise to introduce a new basis, in which the symmetry operators appear in their most clear-cut form.

A change of basis can be achieved by the linear transformation

$$\mathbf{A} = \mathbf{T}\mathbf{A}', \quad \mathbf{B} = \mathbf{T}\mathbf{B}', \quad (9)$$

where the prime now denotes the quantities with respect to the new coordinate system. The matrices  $\mathbf{D}'(P)$  representing the symmetry operators in the new basis are given by the similarity transformation

$$\mathbf{D}'(P) = \mathbf{T}^{-1} \mathbf{D}(P) \mathbf{T}. \quad (10)$$

Likewise the scattering matrix in the new basis becomes

$$\mathbf{S}' = \mathbf{T}^{-1} \mathbf{S} \mathbf{T}. \quad (11)$$

The quantity  $S'$  is a scattering matrix in so far that it relates outgoing waves to incident waves. Its physical meaning cannot always be visualized easily.

The specific transformation matrix  $T$  that is most useful here is the one for which  $D'(P)$  is a completely reduced representation. The matrices  $D'(P)$  will then consist of a set of square submatrices on the principal diagonal, all other submatrices being zero. Thus

$$D'(P) = \begin{bmatrix} D_1(P) & 0 & 0 & \dots \\ 0 & D_2(P) & 0 & \dots \\ 0 & 0 & D_3(P) & \dots \\ \vdots & \vdots & \vdots & \ddots \end{bmatrix}. \quad (12)$$

The dimension of each submatrix in eq. (12) is independent of  $P$ .

It is clear that in this specific basis, called symmetry basis, the coordinates  $A'$  fall apart in a number of subsets, each of which is invariant with respect to all operations  $P$ . The number of elements of any subset equals the dimension of the corresponding irreducible representation.

As  $D(P)$  and  $S$  are subject to the same similarity transformation, eq. (8) is equally valid in the new coordinate system as in the original basis, so that

$$D'(P)S' = S'D'(P), \quad (13)$$

where  $D'(P)$  is given by eq. (12). To evaluate the matrix products in eq. (13) we write

$$S' = \begin{bmatrix} S'_{11} & S'_{12} & S'_{13} & \dots \\ S'_{21} & S'_{22} & S'_{23} & \dots \\ S'_{31} & S'_{32} & S'_{33} & \dots \\ \vdots & \vdots & \vdots & \ddots \end{bmatrix}. \quad (14)$$

Here  $S'$  has been split up into submatrices by identical dividing lines as have been used in eq. (12). The submatrices on the diagonal will therefore be square; the off-diagonal submatrices are in general rectangular, as the various irreducible representations may have different dimensions. Combining eqs (12)-(14) we obtain

$$\begin{bmatrix} D_1S'_{11} & D_1S'_{12} & D_1S'_{13} & \dots \\ D_2S'_{21} & D_2S'_{22} & D_2S'_{23} & \dots \\ D_3S'_{31} & D_3S'_{32} & D_3S'_{33} & \dots \\ \vdots & \vdots & \vdots & \ddots \end{bmatrix} = \begin{bmatrix} S'_{11}D_1 & S'_{12}D_2 & S'_{13}D_3 & \dots \\ S'_{21}D_1 & S'_{22}D_2 & S'_{23}D_3 & \dots \\ S'_{31}\bar{D}_1 & S'_{32}\bar{D}_2 & S'_{33}\bar{D}_3 & \dots \\ \vdots & \vdots & \vdots & \ddots \end{bmatrix}. \quad (15)$$

Though for simplicity it has not been indicated explicitly, eq. (15) is valid for all  $P$ . The separate equations contained in eq. (15) all have the form

$$D_k S'_{kl} = S'_{kl} D_l . \quad (16)$$

Because the matrices  $D'(P)$  are completely reduced, Schur's Lemma applies to eq. (16). This fundamental theorem states, that a matrix  $S'_{kl}$  satisfying eq. (16) for all  $P$  is either (i) a multiple of the unit matrix, if  $D_k$  and  $D_l$  are the same irreducible representations, or (ii) identically zero, if the irreducible representations  $D_k$  and  $D_l$  are non-equivalent. To bring out most clearly the consequences of this theorem we rearrange the irreducible representations in eq. (12) so that

$$D'(P) = \begin{bmatrix} D_1 & 0 & & \\ D_1 & D_1 & 0 & \\ & & D_2 & 0 \\ 0 & & D_2 & D_2 \\ & & 0 & D_3 \\ & & & D_3 \end{bmatrix}, \quad (17)$$

where the subscript now denotes the species of the irreducible representation. Symbolically we can write  $D'(P)$  as the direct sum of its irreducible components, viz.

$$D'(P) = n_1 D_1 + n_2 D_2 + \dots + n_i D_i + \dots \quad (18)$$

The coefficient  $n_i$  denotes the number of times the irreducible representation  $D_i$  occurs in  $D'(P)$ .

If the submatrices in  $\mathbf{S}'$  are ordered in the same fashion as in  $\mathbf{D}'(P)$ , eq. (17),  $\mathbf{S}'$  becomes, by Schur's Lemma,

$$S' = \begin{bmatrix} S_{11}(1) & S_{12}(1) & \cdots & & \\ S_{21}(1) & S_{22}(1) & \cdots & & \\ \vdots & \vdots & \ddots & & \\ & & & S_{n_1 n_1}(1) & \\ & & & & S_{11}(2) \\ & 0 & & & \vdots & \ddots \\ & & & & S_{n_2 n_2}(2) & \\ & & & & & S_{11}(3) \end{bmatrix}. \quad (19)$$

It is seen that a considerable number of submatrices in  $S'$  necessarily vanishes, while all non-zero submatrices  $S_{kl}(i)$  are multiples of the unit matrix. Thus

$$S_{kl}(i) = s_{kl}(i) \mathbf{I}, \quad (20)$$

where  $s_{kl}(i)$  is a number. Hence, the number of constants needed to specify  $S'$  is reduced, by symmetry reasons alone, from  $N^2$  ( $N$  is the number of output leads of the junction) to

$$n_1^2 + n_2^2 + \dots + n_i^2 + \dots \quad (21)$$

No use has been made so far of any of the properties of  $S'$  previously derived, such as the requirements for reciprocity ( $S = \tilde{S}$ ) or for the absence of losses ( $\tilde{S} S^* = \mathbf{I}$ ). Fulfilment of additional conditions like these will in general still further reduce the above number.

Summarizing we can state that the division of the coordinates  $A'$  of the symmetry basis into invariant subsets is less far-reaching with respect to the scattering matrix  $S'$  than with respect to the reduced-out representation of the symmetry group. In fact the number of invariant subsets equals in the former case the number of *different* irreducible representations, whilst in the latter case it is equal to the *total number* of irreducible representations contained in the representation of the group.

The construction of the reduced-out representation, eq. (17), and of the matrix  $T$  needed in the similarity transformations, eqs (10) and (11), will now be outlined very briefly.

Character tables for the crystallographic groups can be found in many texts<sup>9), 11)</sup>. The number of times each irreducible representation appears in the specific representation of the group for the problem on hand can be calculated by a well-known theorem of group theory, involving the characters. The irreducible representations themselves have not been tabulated, but they can in most cases easily be constructed as they are implicitly determined by their known characters. In this way the completely reduced representation  $D'(P)$  can be found.

Once both  $D'(P)$  and  $D(P)$  are known, eq. (10) may be used to obtain a set of linear equations for the individual elements of  $T$ . In all cases where one irreducible representation occurs more than once, this set of equations will be found to be insufficient for the determination of all elements of  $T$ . In fact only the division of the symmetry basis into subsets that are invariant with respect to  $S'$ , eq. (19), is fixed, whereas the choice of the specific coordinates within each subset is arbitrary. This indeterminacy is brought out very elegantly in the method given by Eyring, Walter and Kimball<sup>11)</sup> for the calculation of  $T$ , which method furthermore is much less tedious than the solution of eq. (10).

The limited freedom in the choice of  $\mathbf{T}$  may be used with advantage in those cases where it is known a priori that the scattering matrix can be transformed to a diagonal matrix. This is e.g. always possible for a lossless junction the scattering matrix of which has been proved to be unitary. The symmetry basis can then be chosen in such a way that the elements of  $\mathbf{S}'$ , eq. (19), obey the equations

$$|s_{kk}(i)| = 1; \quad s_{kl}(i) = 0, \quad k \neq l. \quad (21)$$

for all  $i$ .

### III. 3. Field distribution in a symmetry plane

By the adoption of the scattering matrix for the description of waveguide junctions we have deliberately relinquished the aim to obtain any information on the field distribution inside the junction. One is forced to accept this for most practical junctions because of the usually unsurmountable mathematical difficulties encountered in the process of solving Maxwell's equations subject to the boundary conditions imposed by the structure.

The symmetry of a junction can, however, provide us with some knowledge about the field in the interior; in particular some information can be obtained about the distribution in a symmetry plane, point or axis of those fields that correspond to the individual coordinates of the symmetry basis. The insight gained in this respect, though scanty, sometimes enables us to predict qualitatively the effect of alterations in the structure that change the boundary conditions in the symmetry plane, point or axis.

We shall now work out in detail the properties of the field in a symmetry plane, referring the reader for the results in a symmetry point or axis to Dicke<sup>1).</sup>

As reflection in a plane, applied twice in succession, leaves everything unchanged, it constitutes together with the identity operator a group. This group (elements  $I$  and  $F$ ) has two one-dimensional irreducible representations, which obviously are the trivial and the alternating representations. Thus we have

$$D_1(I) = 1, \quad D_1(F) = 1; \quad (22)$$

$$D_2(I) = 1, \quad D_2(F) = -1. \quad (23)$$

The representations eqs (22) and (23) correspond to the familiar concept of solutions even and odd respectively with respect to the symmetry plane. In fig. 3.1 these two different types of solution are illustrated for the electric field vector. Let the field vector on the left-hand side of the symmetry plane be resolved into a component  $E_n$  normal to the plane and a component  $E_t$  parallel to it. The corresponding components of the field

vector on the right-hand side at a symmetrical location are marked with a prime. The following properties can be read from fig. 3.1.

Even solution,  $D_1(F) = +1$ :

$$E_t = E'_t, \quad E_n = -E'_n. \quad (24)$$

Odd solution,  $D_2(F) = -1$ :

$$E_t = -E'_t, \quad E_n = E'_n. \quad (25)$$

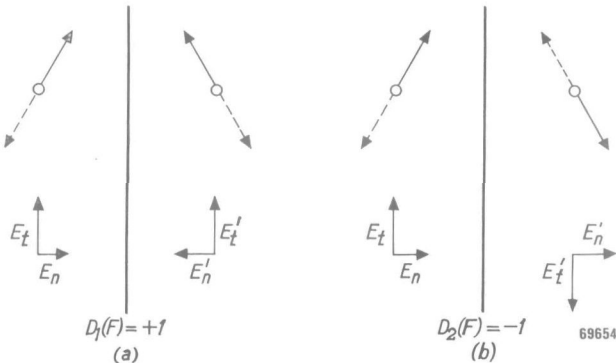


Fig. 3.1. Diagram illustrating an even electric field distribution (a) and an odd distribution (b).

The components of the magnetic field obey equations similar to eqs (24) and (25) but with opposite sign. It should be realized in this connection that the electric field vector is a polar vector, whereas the magnetic field vector is an axial vector (or pseudovector)<sup>12</sup>). Thus we have:

Even solutions,  $D_1(F) = +1$ :

$$H_t = -H'_t, \quad H_n = H'_n. \quad (26)$$

Odd solutions,  $D_2(F) = -1$ :

$$H_t = H'_t, \quad H_n = -H'_n. \quad (27)$$

Equations (24) - (27) are valid for all pairs of points symmetrically located with respect to the symmetry plane, in particular also for the points lying in this plane. The field components with and without a prime become identical there. Hence the electromagnetic field must satisfy the following conditions in the symmetry plane.

Even solutions,  $D_1(F) = +1$ :

$$E_n = 0, \quad H_t = 0. \quad (28)$$

Odd solutions,  $D_2(F) = -1$ :

$$E_t = 0, \quad H_n = 0. \quad (29)$$

The requirements expressed in eq. (28) are identical with the boundary conditions on a perfect conductor. This means that the even solution can be constructed with the aid of eqs (24) and (26) from the solution of Maxwell's equations for the space on one side only of the symmetry plane, which for this purpose is to be covered with a perfectly conducting layer. It may be said that the symmetry plane behaves in the even solution as an electric wall. Analogously for the odd solution the symmetry plane can be described as a magnetic wall, the properties of which are given by eq. (29).

The group  $(I, F)$  will be a subgroup of any point-symmetry group in which the element  $F$  occurs. In the one-dimensional irreducible representations of these groups the representation of  $I$  and  $F$  will necessarily be given either by eq. (22) or by eq. (23). Hence the results derived above apply also in this case.

## CHAPTER IV. JUNCTIONS OF FOUR WAVEGUIDES WITH TWO-FOLD PLANAR SYMMETRY

### IV. 1. The general case

In this and the following chapters we shall discuss junctions of four waveguides which have a structural symmetry that may be termed two-fold planar. The structures possess two mutually perpendicular symmetry planes; their intersection is a two-fold symmetry axis. The crystallographic notation for the group comprising these symmetry operators is  $C_{2v}$ .

Hollow waveguides used in microwave circuits have almost invariably a rectangular cross-section. The lowest mode they can support is the  $TE_{10}$ -mode. We may recall that the field of this mode has only one (transverse) electric component, one transverse magnetic component and a longitudinal magnetic component. These components vary sinusoidally over the width of the guide and are independent of its height. In fig. 4.1 they are illustrated by arrows in the position of their respective maxima.

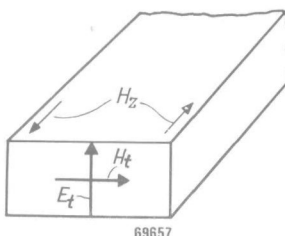


Fig. 4.1. Field components of the  $TE_{10}$ -mode in a rectangular waveguide.

A junction of rectangular waveguides displaying the required symmetry is shown in fig. 4.2. The transverse electric field components, which serve as a basis for the description, have been indicated by arrows. It is of course understood that the interior of the junction is consistent with the symmetry conditions. The two symmetry planes and the symmetry axis have been designated by the letters  $F_1$ ,  $F_2$  and  $R$  respectively, which symbols will be used also to denote the corresponding symmetry operators.

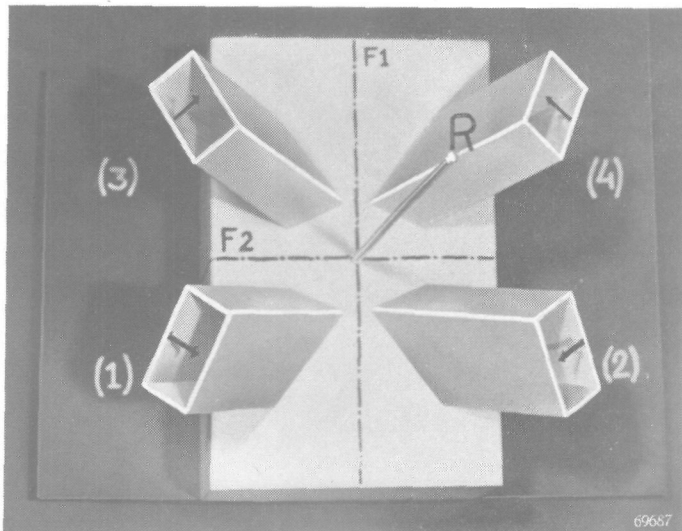


Fig. 4.2. Waveguide junction having two-fold planar symmetry.

The group table for the operators  $I$ ,  $F_1$ ,  $F_2$ , and  $R$  is given in table 4.1. There are three non-trivial subgroups, viz.  $(I, F_1)$ ,  $(I, F_2)$  and  $(I, R)$ .

Table 4.1 Group table

$I$	$F_1$	$F_2$	$R$
$F_1$	$I$	$R$	$F_2$
$F_2$	$R$	$I$	$F_1$
$R$	$F_2$	$F_1$	$I$

The matrices that indicate how the terminal fields interchange when subjected to a symmetry operator can be found by inspection from fig. 4.2. The operator  $F_1$  e.g. permutes the fields in leads (1) and (2) and also the fields in leads (3) and (4). In this way we obtain the following representation of the group

$$\mathbf{D}(I) = \begin{pmatrix} 1000 \\ 0100 \\ 0010 \\ 0001 \end{pmatrix}, \mathbf{D}(F_1) = \begin{pmatrix} 0100 \\ 1000 \\ 0001 \\ 0010 \end{pmatrix}, \mathbf{D}(F_2) = \begin{pmatrix} 0010 \\ 0001 \\ 1000 \\ 0100 \end{pmatrix}, \mathbf{D}(R) = \begin{pmatrix} 0001 \\ 0010 \\ 0100 \\ 1000 \end{pmatrix}. \quad (1)$$

Because the group is Abelian, each element forms a class by itself. The number of irreducible representations, which equals the number of classes, must hence be four. They are all one-dimensional and therefore identical with their characters.

It is to be noted that by a judicious choice of the numbering of the output leads and the direction of the terminal field eq. (1) can be identified with the regular representation of the group. In group theory it is shown that the regular representation contains all irreducible representations a number of times equal to their respective dimensions. The completely reduced form of the representation, eq. (1), must therefore consist of the four one-dimensional irreducible representations. The characters of the

Table 4.2 Character table

	$I$	$F_1$	$F_2$	$R$
$D_1$	1	1	1	1
$D_2$	1	-1	1	-1
$D_3$	1	1	-1	-1
$D_4$	1	-1	-1	1

group  $C_{2v}$  are given in table 4.2. The reduced representation  $\mathbf{D}'(P)$ , which is given by

$$\mathbf{D}'(P) = \begin{pmatrix} D_1(P) & 0 & 0 & 0 \\ 0 & D_2(P) & 0 & 0 \\ 0 & 0 & D_3(P) & 0 \\ 0 & 0 & 0 & D_4(P) \end{pmatrix}, \quad (2)$$

can be written down immediately from table 4.2. We have

$$\mathbf{D}'(I) = \begin{pmatrix} 1 & 0 & 0 & 0 \\ 0 & 1 & 0 & 0 \\ 0 & 0 & 1 & 0 \\ 0 & 0 & 0 & 1 \end{pmatrix}, \mathbf{D}'(F_1) = \begin{pmatrix} 1 & 0 & 0 & 0 \\ 0 & -1 & 0 & 0 \\ 0 & 0 & 1 & 0 \\ 0 & 0 & 0 & -1 \end{pmatrix},$$

$$\mathbf{D}'(F_2) = \begin{pmatrix} 1 & 0 & 0 & 0 \\ 0 & 1 & 0 & 0 \\ 0 & 0 & -1 & 0 \\ 0 & 0 & 0 & -1 \end{pmatrix}, \mathbf{D}'(R) = \begin{pmatrix} 1 & 0 & 0 & 0 \\ 0 & -1 & 0 & 0 \\ 0 & 0 & -1 & 0 \\ 0 & 0 & 0 & 1 \end{pmatrix}. \quad (3)$$

Because the matrices  $\mathbf{D}'(P)$  are diagonal, the scattering matrix transformed to the symmetry basis must also be diagonal. Hence let

$$S' = \begin{pmatrix} s_1 & 0 & 0 & 0 \\ 0 & s_2 & 0 & 0 \\ 0 & 0 & s_3 & 0 \\ 0 & 0 & 0 & s_4 \end{pmatrix}. \quad (4)$$

The matrix  $S'$  is purely diagonal as a consequence of symmetry only; in particular the validity of eq. (4) does not require that the junction should be lossless.

The transformation matrix  $T$  that connects  $S'$ , eq. (4), with the scattering matrix  $S$  can in this specific problem be found in a very direct manner by the following considerations. As the representation, eq. (1), is regular, the symmetry basis for the field description is abstractly identical with the basis in which the group algebra appears as the sum of its invariant subalgebras. We can construct this basis by taking the sum over the group of the products of the complex conjugate of each element of the irreducible representations and the corresponding operator. It thus follows that the elements of  $T$  are proportional to the (real) elements of the irreducible representations, which are given in table 4.2. Contrary to the characters, which have been normalized to the order of the group,  $T$  is normalized to unity so that

$$T = \frac{1}{2} \begin{pmatrix} 1 & 1 & 1 & 1 \\ 1 & -1 & 1 & -1 \\ 1 & 1 & -1 & -1 \\ 1 & -1 & -1 & 1 \end{pmatrix}. \quad (5)$$

By the order in which the characters have been written down in table 4.2  $T$  is a symmetrical matrix. Being orthogonal as well it has the useful property

$$T = \tilde{T} = T^{-1}. \quad (6)$$

The calculation of  $S$  is now a simple matter. By eq. (III.11) we have

$$S = TS'T^{-1}. \quad (7)$$

Substituting eqs (4) and (5) in eq. (7) we obtain after evaluating the matrix product

$$S = \begin{pmatrix} \alpha & \beta & \gamma & \delta \\ \beta & \alpha & \delta & \gamma \\ \gamma & \delta & \alpha & \beta \\ \delta & \gamma & \beta & \alpha \end{pmatrix}, \quad (8)$$

where

$$\left. \begin{aligned} \alpha &= \frac{1}{4}(s_1 + s_2 + s_3 + s_4), \\ \beta &= \frac{1}{4}(s_1 - s_2 + s_3 - s_4), \\ \gamma &= \frac{1}{4}(s_1 + s_2 - s_3 - s_4), \\ \delta &= \frac{1}{4}(s_1 - s_2 - s_3 + s_4). \end{aligned} \right\} \quad (9)$$

#### IV. 2. The nature of the solution

Having completed the mathematical derivation we do well to investigate the physical meaning of the solution. The result that the scattering matrix  $S$ , eq. (8), contains only four different elements could have been deduced directly from inspection of fig. 4.2. The replacement of these four elements by four other unknown constants  $s_n$  as given by eqs (9) is in itself trivial. It is possible, however, to obtain some information on the nature of these constants  $s_n$ . We note that they can be interpreted as reflection coefficients, because they are diagonal elements of the scattering matrix  $S'$ . Each coefficient  $s_n$  belongs to one coordinate of the symmetry basis. The symmetry species of each coordinate can be found in the character table. Recalling the contents of Sec. III.3 we see, e.g., that the electromagnetic field which is invariant if operated on by the irreducible representation  $D_2$  is odd with respect to  $F_1$  and even with respect to  $F_2$ . In other words, the quantity  $s_2$  is the reflection coefficient that would appear in anyone of the output leads if an electric wall had been inserted in plane  $F_1$  and a magnetic wall in plane  $F_2$ . Similar statements can be made for the other symmetry coordinates. The result is shown in diagrammatical form in fig. 4.3, where the quadrant of the junction containing lead (1) is depicted, in a cross-section perpendicular to the planes  $F_1$  and  $F_2$ .

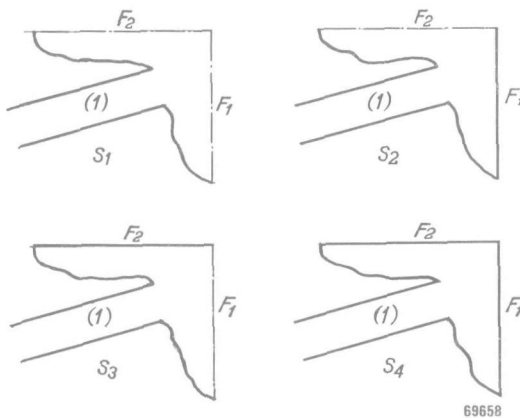


Fig. 4.3. Diagram illustrating the nature of the symmetry planes for the various symmetry coordinates; — · · · — = magnetic wall; — — — = electric wall.

#### IV. 3. The degenerate case

In the two preceding sections the only essential condition imposed on the structure was the two-fold planar symmetry. We shall now discuss a class of junctions which is often met in practical circuits. The geometry

is particularly simple. The junction consists of two straight sections of rectangular waveguide which have one of their side walls in common. The two possible configurations, shown in figs 4.4 and 4.5, are clearly special

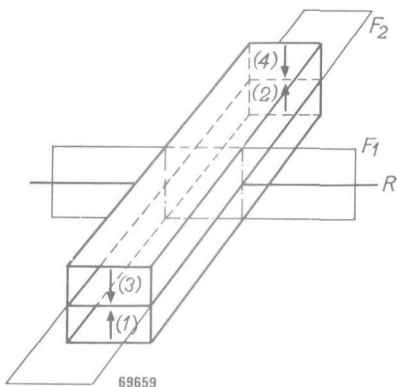


Fig. 4.4. Two sections of rectangular waveguide having one of their wide sides in common.

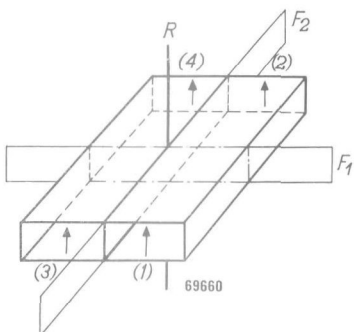


Fig. 4.5. Two sections of rectangular waveguide having one of their narrow sides in common.

cases of the more general junction shown in fig. 4.2. The common wall is assumed to be infinitely thin; this condition is of course never fulfilled in practical structures, but it is often closely approximated. Only discontinuities lying wholly in the common wall are permitted. They can consist e.g. of holes or slots, possibly filled with some dielectric material. Their location and shape are arbitrary, but must be consistent with the symmetry requirements. This means simply that they must be symmetrical with respect to an axis R. Two possible configurations of this kind with circular holes in the common wall are shown in fig. 4.6.

It is possible to obtain more information on the junctions just described than on the more general types discussed in the previous sections, because one of the symmetry planes, viz. F<sub>2</sub>, coincides with a side wall of the wave-

guides. A symmetry plane is known to behave with respect to the field distributions of the coordinates of the symmetry basis either as a perfect electric or a perfect magnetic conductor. The former case clearly imposes the same boundary conditions as the wall of an ideal waveguide. The effect of the discontinuities, lying in the symmetry plane, therefore vanishes for the solutions odd with respect to  $F_2$ ; the junction then degenerates into two independent sections of waveguide. This happens for the irreducible representations  $D_3$  and  $D_4$ , in which the operator  $F_2$  is represented by  $-1$ ,

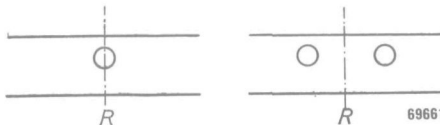


Fig. 4.6. Two examples of coupling holes in the common wall between two waveguides with the symmetry axis  $R$ .

as can be seen from table 4.2. The boundary conditions for the fields described by the reflection coefficients  $s_3$  and  $s_4$  are thus completely specified: an ideal waveguide terminated, for  $s_3$ , by a magnetic short-circuit ( $D_3(F_1) = 1$ ) and, for  $s_4$ , by an electric short-circuit ( $D_4(F_1) = -1$ ). To express the value of  $s_3$  and  $s_4$  numerically we must fix the reference planes; an obvious choice is the symmetry plane  $F_1$  itself. With reference to condition (vi), Sec. I.1, it should be realized that in actual junctions the output leads should be made long enough so that higher modes excited by the discontinuities are sufficiently attenuated before reaching another discontinuity in one of the leads. As the definition of the scattering matrix is based on the transverse electric field, the reflection coefficient of an electric short-circuit is  $-1$  if referred to the position of the short-circuit itself. Analogously for a magnetic short-circuit it equals  $+1$ . Hence

$$s_3 = +1, \quad s_4 = -1. \quad (10)$$

It is thus seen that this special type of junction of four rectangular waveguides can be described by only two constants instead of the four needed for the more general structure with two-fold planar symmetry. Equations (10) inserted in eqs (9) yield

$$\left. \begin{aligned} \alpha &= \frac{1}{4}(s_1 + s_2) \\ \beta &= \frac{1}{4}(s_1 - s_2 + 2) \\ \gamma &= \frac{1}{4}(s_1 + s_2) \\ \delta &= \frac{1}{4}(s_1 - s_2 - 2) \end{aligned} \right\}, \quad (11)$$

Between these four quantities there now exist two relations, viz.

$$\alpha = \gamma \quad \text{and} \quad \beta - \delta = 1. \quad (12)$$

If the junction is lossless,

$$|s_n| = 1. \quad (13)$$

The behaviour of the junction can in this case be specified completely by two real constants, preferably the phase angles of  $s_1$  and  $s_2$ .

It is useful to determine the values of  $s_1$  and  $s_2$  in the limit of infinitely weak coupling between the two sections of waveguide. In the absence of discontinuities the junction simply consists of two sections of ideal waveguide. With the same arguments as used in the derivation of eqs (10) we can write immediately (cf. table 4.2)

$$\begin{aligned} D_1(F_1) &= +1, & s_1 &= +1, \\ D_2(F_1) &= -1, & s_2 &= -1. \end{aligned} \quad (14)$$

As a check on the truth of this result we may note that insertion of eqs (14) in eqs (11) makes all elements vanish except  $\beta$ , which becomes equal to 1. As  $\beta$  denotes the transmission coefficient between leads (1) and (2) and between leads (3) and (4), this result is seen to be correct.

If the junction is lossless and the coupling is weak, the first-order approximation will add small imaginary terms to the unperturbed values of  $s_1$  and  $s_2$ , eqs (14), as follows from eq. (13). Then  $a$ ,  $\gamma$  and  $\delta$  will be small imaginary quantities. A method to calculate these quantities explicitly has been developed by Bethe in his well-known paper on the diffraction by small holes<sup>13)</sup> and in several reports<sup>14), 15)</sup>.

#### IV. 4. The wave matrix

Close inspection of eqs (8) and (11) reveals that it is worth while to introduce a new basis in which the simple properties of the junction are particularly well illustrated. These new coordinates are proportional to the sum and the difference of the wave amplitudes in leads (1) and (3) and in leads (2) and (4). The matrix  $U$  that performs the transformation from the original to the new coordinates is given by

$$U = \frac{1}{\sqrt{2}} \begin{pmatrix} 1 & 0 & 1 & 0 \\ 0 & 1 & 0 & 1 \\ 1 & 0 & -1 & 0 \\ 0 & 1 & 0 & -1 \end{pmatrix}. \quad (15)$$

It is seen to be orthogonal, symmetrical and normalized to unity. As a consequence all the general results derived in Chap. I will be valid for the scattering matrix as transformed to the new basis, which we will call two-mode basis (see below).

The incident waves in terms of the new coordinates are given by (cf. eq. (III.9))

$$A_{im} = \mathbf{U}^{-1} \mathbf{A} = \frac{1}{\sqrt{2}} \begin{pmatrix} 1 & 0 & 1 & 0 \\ 0 & 1 & 0 & 1 \\ 1 & 0 & -1 & 0 \\ 0 & 1 & 0 & -1 \end{pmatrix} \begin{pmatrix} a_1 \\ a_2 \\ a_3 \\ a_4 \end{pmatrix} = \frac{1}{\sqrt{2}} \begin{pmatrix} a_1 + a_3 \\ a_2 + a_4 \\ a_1 - a_3 \\ a_2 - a_4 \end{pmatrix}, \quad (16)$$

and analogously for the emergent waves  $\mathbf{B}_{tm}$ . The scattering matrix  $S_{tm}$  in the two-mode basis is connected to  $\mathbf{S}$  by (cf. eq. (III. 11))

$$S_{tm} = \mathbf{U}^{-1} \mathbf{S} \mathbf{U}. \quad (17)$$

Evaluating the matrix product we find with the aid of eqs (8) and (12)

$$S_{tm} = \begin{pmatrix} \alpha + \gamma & \beta + \delta & 0 & 0 \\ \beta + \delta & \alpha + \gamma & 0 & 0 \\ 0 & 0 & 0 & 1 \\ 0 & 0 & 1 & 0 \end{pmatrix}. \quad (18)$$

In terms of  $s_1$  and  $s_2$  as given by eq. (11) this becomes

$$S_{tm} = \begin{pmatrix} \frac{1}{2}(s_1 + s_2) & \frac{1}{2}(s_1 - s_2) & 0 & 0 \\ \frac{1}{2}(s_1 - s_2) & \frac{1}{2}(s_1 + s_2) & 0 & 0 \\ 0 & 0 & 0 & 1 \\ 0 & 0 & 1 & 0 \end{pmatrix}. \quad (19)$$

The matrix  $S_{tm}$  is seen to be decomposed. The new basis hence comprises two invariant subsets. The fields corresponding to the third and fourth coordinates are purely traveling waves as is evident from the submatrix on the lower right in eq. (19). Only the other subset, containing the first and second coordinates, is affected by the presence of the discontinuities. This suggests the following physical picture. Let us consider the junction as one section of waveguide which can support two modes of propagation instead of two sections of waveguide each capable of supporting only one mode. Each subset of the new coordinates corresponds to one mode. The fields of the first subset (the +mode) are proportional to the sum of the original basis fields; the second subset (the -mode) deals with the difference of the original fields. The fields of these two modes are schematically shown in fig. 4.7. It is clear that the - mode is in no way affected by the presence or removal of the wall separating the two original guides. Discontinuities in this wall will influence only the + mode to an extent given by the submatrix in the upper left corner of  $S_{tm}$ , eq. (19). This submatrix is, indeed, seen to have the form that belongs to a symmetrical obstacle in a waveguide.

The introduction of the two-mode basis is especially useful in problems concerning junctions connected in cascade. Assume e.g. that the two waveguides are coupled by a number of holes spaced apart in the common wall,

each of them satisfying the symmetry requirements. If then we want to express the combined effect in terms of the parameters of the individual discontinuities, the transformation to the two-mode basis reduces the problem to the treatment of two separate waveguides: one loaded by the discontinuities and the other completely unaffected by them<sup>16)</sup>. The scattering matrix, which relates emergent to incident waves, is not suited for the description of junctions connected in cascade. For this purpose we want to express the wave amplitudes on one side of a junction in terms of the amplitudes on the other side. In our case this amounts to a relation between the amplitudes in guides (1) and (3) and the amplitudes in guides (2) and (4). The matrix describing the connection between these quantities has been termed the wave matrix<sup>17)</sup>. The main point in the use of this matrix is that the wave matrix of a series of discontinuities equals simply the product of the wave matrices of the individual discontinuities taken in the proper order.

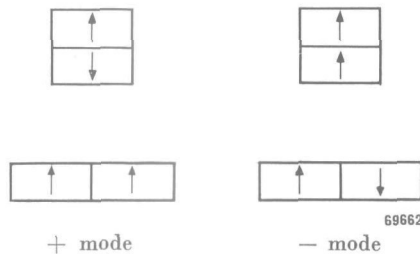


Fig. 4.7. Schematic representation of two modes of propagation.

We shall derive the wave matrix only in the two-mode basis. We first reproduce the scattering description explicitly. By eqs (16) and (19) we have

$$\frac{1}{\sqrt{2}} \begin{pmatrix} b_1 + b_3 \\ b_2 + b_4 \\ b_1 - b_3 \\ b_2 - b_4 \end{pmatrix} = \begin{pmatrix} \frac{1}{2}(s_1 + s_2) & \frac{1}{2}(s_1 - s_2) & 0 & 0 \\ \frac{1}{2}(s_1 - s_2) & \frac{1}{2}(s_1 + s_2) & 0 & 0 \\ 0 & 0 & 0 & 1 \\ 0 & 0 & 1 & 0 \end{pmatrix} \frac{1}{\sqrt{2}} \begin{pmatrix} a_1 + a_3 \\ a_2 + a_4 \\ a_1 - a_3 \\ a_2 - a_4 \end{pmatrix}. \quad (20)$$

By an elementary calculation the above four linear equations can be rearranged so as to bring all wave amplitudes with subscripts 2 and 4 on the left-hand side. We find

$$\frac{1}{\sqrt{2}} \begin{pmatrix} b_2 + b_4 \\ a_2 + a_4 \\ b_2 - b_4 \\ a_2 - a_4 \end{pmatrix} = \begin{pmatrix} \frac{2s_1s_2}{s_1 - s_2} & \frac{s_1 + s_2}{s_1 - s_2} & 0 & 0 \\ -\frac{s_1 + s_2}{s_1 - s_2} & \frac{2}{s_1 - s_2} & 0 & 0 \\ -\frac{s_1 - s_2}{s_1 - s_2} & \frac{s_1 - s_2}{s_1 - s_2} & 0 & 0 \\ 0 & 0 & 1 & 0 \\ 0 & 0 & 0 & 1 \end{pmatrix} \frac{1}{\sqrt{2}} \begin{pmatrix} a_1 + a_3 \\ b_1 + b_3 \\ a_1 - a_3 \\ b_1 - b_3 \end{pmatrix}. \quad (21)$$

Like the scattering matrix the wave matrix in eq. (21) is, of course, decomposed. The two elements 1 on the diagonal clearly demonstrate again that the —mode is unaffected by the discontinuities.

#### IV. 5. Shift of the reference planes

If it is desirable to describe the behaviour of the junction with reference to planes other than the symmetry plane  $F_2$ , it should be realized that the new planes must all be equidistant from  $F_2$  for reasons of symmetry. The matrix  $\Phi$  needed in the transformation of the scattering matrix  $S$  (cf. Sec. I.4) therefore has the almost-trivial form

$$\Phi = e^{i\varphi} \mathbf{I}, \quad (22)$$

where  $\varphi = \beta l$  is the phase angle corresponding to an outward shift over a distance  $l$ . Denoting with a prime the quantities with respect to the new reference planes we simply have

$$S' = e^{2i\varphi} S. \quad (23)$$

To investigate the required transformation for the wave matrix we rewrite eq. (21). We have

$$C_{24} = W C_{13}, \quad (24)$$

where the column matrices of eq. (21) have been denoted by  $C_{24}$  and  $C_{13}$ ;  $W$  represent the wave matrix. The column matrices transform according to

$$C'_{24} = \Psi C_{24}, \quad C'_{13} = \Psi^{-1} C_{13}, \quad (25)$$

where

$$\Psi = \begin{pmatrix} e^{i\varphi} & 0 & 0 & 0 \\ 0 & e^{-i\varphi} & 0 & 0 \\ 0 & 0 & e^{i\varphi} & 0 \\ 0 & 0 & 0 & e^{-i\varphi} \end{pmatrix}, \quad (26)$$

as follows from the properties of the individual elements of  $C_{24}$  and  $C_{13}$ . Substitution of eq. (25) in eq. (24) yields

$$W' = \Psi W \Psi.$$

With the aid of eqs (21), (26) and (27) we can construct the wave matrix  $W'$  with respect to the new terminal planes explicitly; it is found to be

$$W' = \begin{pmatrix} -\frac{2s'_1 s'_2}{s'_1 - s'_2} & \frac{s'_1 + s'_2}{s'_1 - s'_2} & 0 & 0 \\ -\frac{s'_1 + s'_2}{s'_1 - s'_2} & \frac{2}{s'_1 - s'_2} & 0 & 0 \\ 0 & 0 & e^{2i\varphi} & 0 \\ 0 & 0 & 0 & e^{-2i\varphi} \end{pmatrix}, \quad (28)$$

where

$$s'_n = s_n e^{2i\varphi}, n = 1, 2. \quad (29)$$

## CHAPTER V. DIRECTIONAL COUPLERS

### V. 1. Condition for perfect directivity

A junction of four waveguides constitutes a directional coupler if the four output leads can be divided into two pairs with the property that no coupling exists between the leads of each pair. Junctions having a scattering matrix  $S$  of the form

$$S = \begin{pmatrix} \alpha & \beta & \gamma & \delta \\ \beta & \alpha & \delta & \gamma \\ \gamma & \delta & \alpha & \beta \\ \delta & \gamma & \beta & \alpha \end{pmatrix} \quad (1)$$

satisfy this definition if one of the transmission coefficients  $\beta$ ,  $\gamma$  or  $\delta$  vanishes. For lossless junctions it can be proved<sup>1)</sup> that this condition necessarily implies

$$\alpha = 0. \quad (2)$$

The converse is true also: if  $\alpha$  vanishes, i.e. if the junction is completely matched, then it is a directional coupler. Hence eq. (2) is a necessary and sufficient condition for a lossless junction to be a directional coupler. This theorem is not limited to junctions described by eq. (1): any completely matched, lossless junction of four waveguides is a directional coupler<sup>18)</sup>.

Let us now consider a lossless junction with two-fold planar symmetry consisting of two parallel sections of rectangular waveguide which have one of their side walls in common. If only discontinuities lying in the common wall, assumed to be infinitely thin, are permitted, the elements of the scattering matrix are given by eqs (IV. 11), viz.

$$\left. \begin{aligned} \alpha &= \frac{1}{4}(s_1 + s_2) \\ \beta &= \frac{1}{4}(s_1 - s_2 + 2) \\ \gamma &= \frac{1}{4}(s_1 + s_2) \\ \delta &= \frac{1}{4}(s_1 - s_2 - 2). \end{aligned} \right\} \quad (3)$$

To recall the physical meaning of the various elements, the waves scattered by the junction are shown schematically in fig. 5.1 for an incident wave in lead (1) only. From now on we confine the discussion to junctions of the type described by eqs (1) and (3).

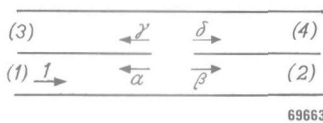


Fig. 5.1. The amplitudes of the scattered waves.

Because

$$\alpha = \gamma, \quad (4)$$

the only way in which the junction can act as a directional coupler ( $\alpha = 0$ ) is the decoupling of lead (3) from lead (1) and of lead (4) from lead (2).

From eqs (2) and (3) it follows that the condition for perfect directivity is equivalent to

$$s_1 + s_2 = 0. \quad (5)$$

With the aid of this equation we can deduce the relevant condition for the wave matrix of a directional coupler. From eq. (IV. 21) it is found that in the two-mode basis the wave matrix of a directional coupler is diagonal. It is evident that a junction with a diagonal wave matrix is matched. In that case the + mode, which in general is partially reflected, only suffers a change of phase in passing the discontinuities.

The two quantities commonly used to specify the behaviour of a directional coupler are the directivity  $D$  and the coupling  $C$ . The former indicates quantitatively how effectively the desired decoupling has been realized. It is defined as the ratio of the power coupled in the wanted direction to the power coupled in the unwanted direction. Expressed in decibels it is for the junction of fig. 5.1 given by

$$D = 20 \log \frac{|\delta|}{|\gamma|}. \quad (6)$$

The coupling  $C$  is defined as the ratio of the incident power to the power split off in the wanted direction. Thus

$$C = -20 \log |\delta|. \quad (7)$$

## V. 2. Bethe-hole coupler

A directional coupler of which the properties seem to be in direct contradiction to the conclusions reached in the preceding section is the well-known Bethe-hole coupler<sup>15), 19), 20)</sup>. It consists of two rectangular waveguides which are coupled by a circular hole in the centre of their common wide side. The small-hole theory indicates that the coefficient  $\delta$  of this junction vanishes if the guide wavelength equals the cut-off wavelength. From eq. (3), however, it follows that for  $\delta = 0$  the quantities  $s_1$  and  $s_2$  necessarily have their unperturbed values +1 and -1 respectively, which situation corresponds to the trivial case of no coupling at all between the two sections of waveguide. The solution of this apparent paradox lies in the fact that Bethe's theory is a first-order approximation; accordingly the coefficient  $\delta$  of a Bethe-hole coupler is not zero but small of the second order as will now be shown.

The junction is assumed to be lossless. Then we may write (cf. eq. (IV.13))

$$s_1 = e^{i\vartheta_1}, \quad s_2 = -e^{i\vartheta_2}, \quad (8)$$

where  $\vartheta_1$  and  $\vartheta_2$  are real. The signs in eqs (8) have been chosen in conformity with eqs (IV. 14) so that for weak coupling the absolute magnitude of both  $\vartheta_1$  and  $\vartheta_2$  is small compared with unity. With the aid of eqs (8) we obtain from eqs (3)

$$|\gamma| = \frac{1}{2} |\sin \frac{1}{2}(\vartheta_1 - \vartheta_2)|, \quad (9)$$

$$|\delta|^2 = \frac{1}{4} [1 + \cos^2 \frac{1}{2}(\vartheta_1 - \vartheta_2) - 2 \cos \frac{1}{2}(\vartheta_1 - \vartheta_2) \cos \frac{1}{2}(\vartheta_1 + \vartheta_2)]. \quad (10)$$

Apparently  $|\gamma|$  is determined by  $(\vartheta_1 - \vartheta_2)$  only, whilst  $|\delta|$  is a function of  $(\vartheta_1 + \vartheta_2)$  as well. Minimizing  $|\delta|$  with respect to the latter quantity we have

$$|\delta|_{\min} = \frac{1}{2} [1 - \cos \frac{1}{2}(\vartheta_1 - \vartheta_2)]. \quad (11)$$

As for small holes

$$|\vartheta_1 - \vartheta_2| \ll 1, \quad (12)$$

the first term of the series expansions for  $|\gamma|$  and  $|\beta|$  are given by

$$|\gamma| \approx \frac{1}{4} |\vartheta_1 - \vartheta_2|, \quad (13)$$

$$|\delta|_{\min} \approx \frac{1}{16} (\vartheta_1 - \vartheta_2)^2. \quad (14)$$

Thus it is seen that  $|\delta|_{\min}$  is small of the second order; in fact  $|\delta|_{\min}$  is just equal to the square of  $|\gamma|$ . In terms of coupling and directivity, which for the Bethe-hole coupler are *not* given by eqs (6) and (7), but rather by  $-20 \log|\gamma|$  and  $20 \log|\gamma/\delta|$  respectively, we can conclude that for this type of coupler the directivity is never greater than the coupling.

### V. 3. Systems of identical junctions connected in cascade

In this section we shall treat waveguide systems obtained by cascading a number of identical junctions. In particular the consequences of the condition for perfect directivity will be investigated.

Our first aim is to express the quantities describing the behaviour of the complete system in terms of the elements of the scattering matrix of the individual junctions. The way to achieve this has been prepared in Sec. IV.4 by the introduction of the wave matrix. It was pointed out there that the wave matrix of a number of junctions in cascade is equal to the product of the wave matrices belonging to each junction individually. If we confine ourselves to systems of  $n$  identical junctions in cascade as shown schematically in fig. 5.2, we have

$$\mathbf{W}'_n = \mathbf{W}'^n. \quad (15)$$

Here  $\mathbf{W}'_n$  represents the wave matrix of the system and  $\mathbf{W}'$  the wave matrix of a single junction. The primes in eq. (15) indicate that the wave

matrices do not refer to the symmetry planes, but rather to the boundary planes between the individual junctions shown in fig. 5.2 by dashed lines. For  $\mathbf{W}'_n$  the reference planes are given by the two outermost planes in fig. 5.2.

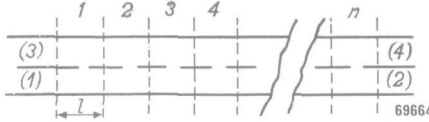


Fig. 5.2. System of  $n$  junctions connected in cascade.

The wave matrix  $\mathbf{W}'$  is given by eq. (IV. 28), viz.

$$\mathbf{W}' = \begin{pmatrix} \frac{2s'_1 s'_2}{s'_1 - s'_2} & \frac{s'_1 + s'_2}{s'_1 - s'_2} & 0 & 0 \\ -\frac{s'_1 + s'_2}{s'_1 - s'_2} & \frac{2}{s'_1 - s'_2} & 0 & 0 \\ 0 & 0 & e^{2i\varphi} & 0 \\ 0 & 0 & 0 & e^{-2i\varphi} \end{pmatrix}, \quad (16)$$

where  $2\varphi$  is the phase angle corresponding to the length  $l$  of each junction. Introducing the phase angles of  $s_1$  and  $s_2$  according to eq. (8) we have by eq. (IV. 29)

$$s'_1 = e^{2i\varphi} s_1 = e^{i(2\varphi + \theta_1)}, \quad s'_2 = e^{2i\varphi} s_2 = -e^{i(2\varphi + \theta_2)}, \quad (17)$$

where  $s_1$  and  $s_2$  are as usual defined with respect to the symmetry plane of an individual junction.

Insertion of eq. (16) in eq. (15) and subsequent evaluation of the  $n$ th power of  $\mathbf{W}'$  yields

$$\mathbf{W}'_n = \begin{pmatrix} \cos n \zeta \pm \frac{1 + s'_1 s'_2 \sin n \zeta}{s'_1 - s'_2} \frac{\sin n \zeta}{\sin \zeta} & \frac{s'_1 + s'_2 \sin n \zeta}{s'_1 - s'_2} \frac{\sin n \zeta}{\sin \zeta} & 0 & 0 \\ -\frac{s'_1 + s'_2 \sin n \zeta}{s'_1 - s'_2} \frac{\sin n \zeta}{\sin \zeta} & \cos n \zeta \mp \frac{1 + s'_1 s'_2 \sin n \zeta}{s'_1 - s'_2} \frac{\sin n \zeta}{\sin \zeta} & 0 & 0 \\ 0 & 0 & e^{2in\varphi} & 0 \\ 0 & 0 & 0 & e^{-2in\varphi} \end{pmatrix}. \quad (18)$$

The auxiliary quantity  $\zeta$  is determined by

$$\cos \zeta = \frac{1 - s'_1 s'_2}{s'_1 - s'_2}. \quad (19)$$

The ambiguity of sign in two elements of  $\mathbf{W}'_n$  arises from the definition of  $\zeta$ , eq. (19), which leaves the sign of  $\zeta$  undetermined. Which sign is the correct one will be apparent at a later stage of the discussion.

In Sec. 1 it has been shown that the wave matrix of a coupler with perfect directivity is diagonal. It follows that the condition for perfect directivity for the system described by  $\mathbf{W}'_n$ , eq. (18), is given by

$$\frac{s'_1 + s'_2}{s'_1 - s'_2} \frac{\sin n\zeta}{\sin \zeta} = 0. \quad (20)$$

Equation (20) has two solutions, viz.

$$s'_1 + s'_2 = 0, \quad (21)$$

and

$$\frac{\sin n\zeta}{\sin \zeta} = 0. \quad (22)$$

We shall first deal with systems obeying eq. (21). By this condition it is required that each individual junction is by itself a directional coupler; the complete system then is a directional coupler irrespective of the number  $n$  of junctions contained in it.

Throughout this chapter we assume that the phase angles  $\vartheta_1$  and  $\vartheta_2$  of the individual junctions, as introduced in eqs (8), are considerably smaller than  $\pi$ . Then the condition for directivity, eq. (21), has only one solution, viz.

$$\vartheta_1 = \vartheta_2 \equiv \vartheta. \quad (23)$$

Let us assume that this condition is fulfilled. Equation (19) now becomes

$$\cos \zeta = \cos (2\varphi + \vartheta), \quad (24)$$

while further

$$\frac{1 + s'_1 s'_2}{s'_1 - s'_2} = -i \sin (2\varphi + \vartheta). \quad (25)$$

By eqs (21), (24) and (25) the wave matrix of the system, eq. (18), takes the simple form

$$\mathbf{W}'_n = \begin{pmatrix} e^{\pm in(2\varphi + \vartheta)} & 0 & 0 & 0 \\ 0 & e^{\mp in(2\varphi + \vartheta)} & 0 & 0 \\ 0 & 0 & e^{2in\varphi} & 0 \\ 0 & 0 & 0 & e^{-2in\varphi} \end{pmatrix}. \quad (26)$$

It is now clear that the upper sign in the exponentials should be taken, as for vanishing  $\vartheta$  the matrix  $\mathbf{W}'_n$  should represent a simple phase shift.

Equation (26) can be written as

$$\mathbf{W}'_n = \begin{pmatrix} e^{in\varphi} & 0 & 0 & 0 \\ 0 & e^{-in\varphi} & 0 & 0 \\ 0 & 0 & e^{in\varphi} & 0 \\ 0 & 0 & 0 & e^{-in\varphi} \end{pmatrix} \begin{pmatrix} e^{in\vartheta} & 0 & 0 & 0 \\ 0 & e^{-in\vartheta} & 0 & 0 \\ 0 & 0 & 1 & 0 \\ 0 & 0 & 0 & 1 \end{pmatrix} \begin{pmatrix} e^{in\varphi} & 0 & 0 & 0 \\ 0 & e^{-in\varphi} & 0 & 0 \\ 0 & 0 & e^{in\varphi} & 0 \\ 0 & 0 & 0 & e^{-in\varphi} \end{pmatrix}. \quad (27)$$

Hence the wave matrix  $\mathbf{W}_n$  referred to the symmetry plane of the system is given by the central matrix in the above product.

The scattering matrix in the two-mode basis  $S_{tm}$  can be derived from  $\mathbf{W}_n$  with the aid of eqs (IV. 20) and (IV. 21). We find

$$S_{tm} = \begin{pmatrix} 0 & e^{in\vartheta} & 0 & 0 \\ e^{in\vartheta} & 0 & 0 & 0 \\ 0 & 0 & 0 & 1 \\ 0 & 0 & 1 & 0 \end{pmatrix}, \quad (28)$$

whence by eq. (IV. 17)

$$\mathbf{S} = \begin{pmatrix} 0 & \beta & 0 & \delta \\ \beta & 0 & \delta & 0 \\ 0 & \delta & 0 & \beta \\ \delta & 0 & \beta & 0 \end{pmatrix}, \quad (29)$$

with

$$\beta = \frac{1}{2}(e^{in\vartheta} + 1), \quad \delta = \frac{1}{2}(e^{in\vartheta} - 1). \quad (30)$$

A graphical representation of  $\beta$  and  $\delta$  is shown in fig. 5.3. The circle is the locus of the end points of the vectors regarded as functions of  $n$ .

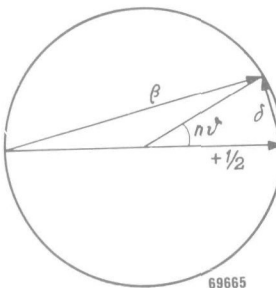


Fig. 5.3. Locus of the transmission coefficients  $\beta$  and  $\delta$  in the complex plane, both as a function of  $n$ .

With increasing  $n$  the radius of the circle rotates counter-clockwise so that alternately  $|\beta|$  and  $|\delta|$  go through zero and a maximum respectively. In a system with  $n\vartheta \gg \pi$ ,  $\vartheta \ll \pi$ , power incident e.g. in lead (1) will be transferred many times to the upper guide and back again to the lower guide before leaving the system by leads (3) and (4). This phenomenon has sometimes been called spatial beating and is known to happen also in parallel waveguides with a long slot in the common wall<sup>20), 21)</sup>.

The conditions corresponding to special values of the coupling can be read directly from fig. 5.3. For equal power partition (e.g.) we must have

$$|\beta| = |\delta| \quad \text{for } n\vartheta = \pi/2, 3\pi/2, 5\pi/2 \dots ; \quad (31)$$

for complete transfer of power from one guide to the other

$$\beta = 0, \quad |\delta| = 1 \quad \text{for } n\vartheta = \pi, 3\pi, 5\pi, \dots \quad (32)$$

The general expression for the coupling  $C$  in terms of  $n\vartheta$  is by eqs (7) and (30)

$$C = -20 \log |\delta| = -20 \log |\sin \frac{1}{2} n\vartheta|. \quad (33)$$

A very effective design for a directional coupler of the type just discussed has been described in a paper by Riblet and Saad<sup>22)</sup>. The discontinuities in the common wide side between the waveguides consist here of two slots: one transverse and one longitudinal with respect to the axes of the waveguides, as shown in fig. 5.4. Because the slots are narrow, coupling by the electric field vector is negligible. With regard to the magnetic coupling we recall that the fields corresponding to  $s_1$  and  $s_2$  are obtained by inserting in the symmetry plane  $F_1$  a magnetic and an electric wall respectively.

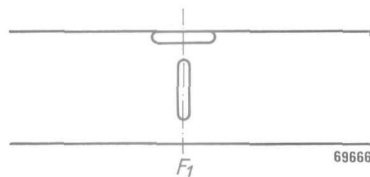


Fig. 5.4. Coupling slots used in directional couplers.

The magnetic wall annuls the coupling through the transverse slot;  $s_1$  therefore is determined only by the size of the longitudinal slot and unaffected by the transverse slot. An electric wall in  $F_1$  places a short circuit across the longitudinal slot, thereby greatly reducing its effect. Hence  $s_2$  is determined almost exclusively by the transverse slot.

For slots short compared with the wavelength the value of  $\vartheta_1$  belonging to the longitudinal slot and the value of  $\vartheta_2$  belonging to the transverse slot can be calculated with the aid of Bethe's theory. For larger slots measurements taken on each slot separately will yield the dependence of  $\vartheta_1$  and  $\vartheta_2$  on slot size. By combination of slots with equal values of  $\vartheta$  a directional coupler is obtained.

Once one pair of slots has been designed so as to give high directivity and the value of  $\vartheta$  is known, the number of junctions needed to give a specified coupling can be calculated with the aid of eq. (33).

As a specific example we quote some results obtained with systems constructed from standard size 3-cm waveguide having  $0.400'' \times 0.900''$  ID. The dimensions of the slots cut in the common wall of thickness 0.500" are given in fig. 5.5. The phase angle of both  $s_1$  and  $s_2$  is ten degrees. The

dependence of the coupling on the number  $n$  of cascaded junctions as calculated from eq. (33) is given for this specific case in table 5.1.

TABLE 5.1

$n$	$ \delta $	C db
1	0.087	21.2
2	0.17	15.2
3	0.26	11.8
4	0.34	9.3
5	0.42	7.5
6	0.50	6.0
9	0.71	3.0
18	1.00	0.0

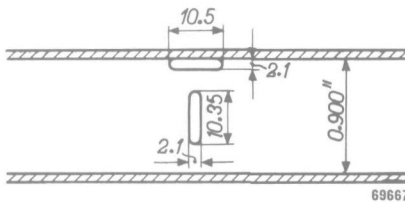


Fig. 5.5. Slot dimensions in millimetres so as to make  $\theta = 10^\circ$  for a frequency of 9400 Mc/s.

We shall limit the investigation of the consequences of the second directivity condition, viz.

$$\frac{\sin n\zeta}{\sin \zeta} = 0, \quad (22)$$

to the practically important case that the two sections of waveguide are coupled by only two identical holes in their common wall. For  $n = 2$  eq. (22) becomes

$$\cos \zeta = 0. \quad (34)$$

Insertion of eqs (22) and (34) in the general expression for the wave matrix eq. (18), yields

$$W'_2 = \begin{pmatrix} -1 & 0 & 0 & 0 \\ 0 & -1 & 0 & 0 \\ 0 & 0 & e^{4i\varphi} & 0 \\ 0 & 0 & 0 & e^{-4i\varphi} \end{pmatrix}. \quad (35)$$

The corresponding scattering matrix is found to be

$$\mathbf{S}' = \begin{pmatrix} 0 & \beta' & 0 & \delta' \\ \beta' & 0 & \delta' & 0 \\ 0 & \delta' & 0 & \beta' \\ \delta' & 0 & \beta' & 0 \end{pmatrix}, \quad (36)$$

with

$$\beta' = -\frac{1}{2}(1 - e^{4i\varphi}), \quad \delta' = -\frac{1}{2}(1 + e^{4i\varphi}). \quad (37)$$

The individual junctions used in this type of coupler are usually completely non-directional. This is the case if either  $s_1$  or  $s_2$  retains its unperturbed value in spite of the presence of the discontinuity. We have seen above that this happens for each of the slots of the junction shown in fig. 5.4. As the field of the lowest mode in a rectangular waveguide is independent of its height, a hole in the narrow side will behave in exactly the same manner as a longitudinal slot cut in the wide side adjacent to the narrow side. Hence for a junction of two rectangular waveguides having a small hole in the common narrow side the value of  $s_2$  is unperturbed so that

$$s_2 = -1, \quad \vartheta_2 = 0. \quad (38)$$

Let us restrict the discussion to two-hole systems obeying eq. (38). By substitution of this equation in the expression for  $\cos \zeta$ , eq.(19), the directivity condition eq. (34) becomes

$$e^{i(4\varphi + \vartheta_1)} + 1 = 0. \quad (39)$$

The smallest root of eq. (39) is given by

$$2\varphi = \frac{1}{2}(\pi - \vartheta_1). \quad (40)$$

Now  $2\varphi$  is the phase angle corresponding to the length of each junction as is also shown in fig. 5.6. Hence it follows from eq. (40) that the distance between the symmetry planes of the individual non-directional junctions should be smaller than a quarter wavelength in a two-hole coupler. The amount of the correction depends on the value of  $\vartheta_1$ , which quantity is decisive for the coupling as will be shown below. With the aid of eq. (39)  $\varphi$  can be eliminated from the expressions for  $\beta'$  and  $\delta'$ , eqs (37). Thus

$$\beta' = -\frac{1}{2}(1 + e^{-i\vartheta_1}), \quad \delta' = -\frac{1}{2}(1 - e^{-i\vartheta_1}). \quad (41)$$

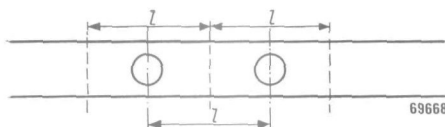


Fig. 5.6. A two-hole coupler.

Referred to the symmetry plane of the complete coupler the relevant quantities are

$$\beta = e^{-2i\vartheta} \quad \beta' = -e^{i\vartheta_1} \quad \beta' = \frac{1}{2}(e^{i\vartheta_1} + 1), \quad (42)$$

and analogously

$$\delta = \frac{1}{2}(e^{i\vartheta_1} - 1). \quad (43)$$

These equations are seen to be identical with eqs (30) for  $n = 1$ . This, indeed, was to be expected, because transducer theory does not discriminate between structures, provided their scattering properties are the same, even if internally they differ radically. Hence if a number of two-hole couplers are connected in cascade, the discussion leading up to eqs (30) is fully applicable; in this fashion the theory for binomial couplers e.g. can be derived.

The coupling  $C$  of a two-hole coupler in terms of  $\vartheta_1$  is given by

$$C = -20 \log |\delta| = -20 \log |\sin \frac{1}{2} \vartheta_1|. \quad (44)$$

Once the transmission through one hole and hence  $\vartheta_1$  has been determined, the correct spacing for a two-hole directional coupler can be calculated from eq. (40) and the coupling to be expected from eq. (44). In fact by substituting eq. (38) in eqs (3) it can be proved that  $|\delta|$  of a two-hole coupler is just twice the absolute value of the transmission coefficient  $\delta$  of a single hole.

In a paper by Rosen and Bangert<sup>23)</sup> the conclusion is reached that with a two-hole coupler perfect directivity can never be achieved. As, however, their theory is founded on Bethe's first-order approximation for the coupling through small holes, their results regarding possible second order effects are not conclusive.

#### V. 4. Frequency dependence of directional couplers

The fundamental theorem derived in Sec. I.7. is the starting-point for the investigation of the frequency dependence of directional couplers. It states that the phase angle of the reflection coefficient of a lossless termination always increases with frequency. As the quantities  $s_1$  and  $s_2$ , which specify the behaviour of couplers of the type discussed, are essentially reflection coefficients, the above theorem applies to them.

The coefficients involved in the definitions of coupling and directivity are given by

$$\gamma = \frac{1}{4}(s_1 + s_2), \quad \delta = \frac{1}{4}(s_1 - s_2 - 2). \quad (45)$$

Note that here  $s_1$  and  $s_2$  refer to the complete system, which may consist of several cascaded junctions.

Let again

$$s_1 = e^{i\vartheta_1}, \quad s_2 = -e^{i\vartheta_2}. \quad (8)$$

Substituting eqs (8) in eqs (45) and differentiating the latter with respect to the angular frequency  $\omega$  we obtain

$$\frac{d\gamma}{d\varphi} = \frac{i}{4} \left( s_1 \frac{d\vartheta_1}{d\omega} + s_2 \frac{d\vartheta_2}{d\omega} \right), \quad \frac{d\delta}{d\omega} = \frac{i}{4} \left( s_1 \frac{d\vartheta_1}{d\omega} - s_2 \frac{d\vartheta_2}{d\omega} \right). \quad (46)$$

If for  $\omega = \omega_0$  the junction is perfectly directional,  $s_2$  can be eliminated from eqs (46) with the aid of eq. (5). Thus

$$\left( \frac{d\gamma}{d\omega} \right)_{\omega_0} = \frac{is_1}{4} \left( \frac{d\vartheta_1}{d\omega} - \frac{d\vartheta_2}{d\omega} \right)_{\omega_0}, \quad \left( \frac{d\delta}{d\omega} \right)_{\omega_0} = \frac{is_1}{4} \left( \frac{d\vartheta_1}{d\omega} + \frac{d\vartheta_2}{d\omega} \right)_{\omega_0}. \quad (47)$$

By the general theorem both

$$\frac{d\vartheta_1}{d\omega} > 0 \quad \text{and} \quad \frac{d\vartheta_2}{d\omega} > 0. \quad (49)$$

Hence it is possible that  $(d\gamma/d\omega)_{\omega_0}$  vanishes, in which case the directivity is broadband. For broadband coupling it is required that  $(d\delta/d\omega)_{\omega_0}$  be perpendicular to  $\delta$ . This can only be achieved in special cases, as can be seen from fig. 5.7. In this diagram the circle is the locus of  $\frac{1}{2}s_1$  and  $\frac{1}{2}s_2$  regarded as a function of frequency. By the general theorem both  $s_1$  and

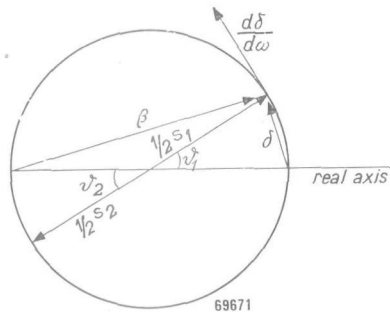


Fig. 5.7. Locus of  $\frac{1}{2}s_1$  and  $\frac{1}{2}s_2$  as a function of frequency.

$s_2$  rotate counter-clockwise with increasing frequency. It is immediately clear that perfect directivity is maintained as long as  $s_1$  and  $s_2$  are exactly opposite. On the other hand it is seen that, as  $(d\delta/d\omega)_{\omega_0}$  is tangent to the circle,  $|\delta|$  necessarily increases with frequency for small values of  $\vartheta$ . However, under conditions for total power transfer, i.e.  $|\delta| = 1$ ,  $\vartheta = \pi$ , the derivative of  $\delta$  with respect to frequency is perpendicular to  $\delta$  and the coupling is broadband.

### V. 5. Variable attenuator \*)

A cascaded directional coupler can be used with advantage as the basic unit for a variable attenuator. In Sec. 3 it has been shown that if the number  $n_0$  of directional couplers connected in cascade obeys the equation

$$n_0\vartheta = \pi, \quad (32)$$

power incident in a lead is completely transferred to the lead diametrically opposite. If now it were possible to vary the number of junctions from  $n_0$  downwards, the transmission through the system could be controlled and the instrument would be a variable attenuator. This, of course, cannot be done, but in a slightly different way the same effect can be achieved.

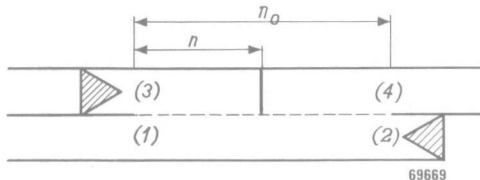


Fig. 5.8. Waveguide system used in a variable attenuator.

Let us consider the system schematically shown in fig. 5.8. A large number  $n_0$  of directional couplers each having a small value of  $\vartheta$  is connected in cascade. Leads (2) and (3) of the system are terminated by matched loads. A partition has been placed in the upper guide between the junctions numbered  $n$  and  $n + 1$  from lead (1). Both faces of the partition are completely absorbing, i.e. non-reflecting for waves incident on it.

The scattering matrix  $S'_n$  for the system comprising the first  $n$  junctions from the left is obtained from eq. (29) by deleting the third and fourth rows and columns because the corresponding leads are terminated by matched loads. Thus

$$S'_n = \begin{pmatrix} 0 & \beta'_n \\ \beta'_n & 0 \end{pmatrix}, \quad (49)$$

with

$$\beta'_n = \frac{1}{2} e^{2in\varphi} (e^{in\vartheta} + 1). \quad (50)$$

Analogously the scattering matrix  $S'_{n_0-n}$  for the system comprising the remaining junctions is found from eq. (29) by omitting the second and third rows and columns. Hence

$$S'_{n_0-n} = \begin{pmatrix} 0 & \delta'_{n_0-n} \\ \delta'_{n_0-n} & 0 \end{pmatrix}, \quad (51)$$

\*) The original ideas underlying the construction of the instruments described in this and the next section are due to Ir. W. J. van de Lindt of Philips Research Laboratories.

where

$$\delta'_{n_0-n} = \frac{1}{2} e^{2i(n_0-n)\vartheta} (e^{i(n_0-n)\vartheta} - 1). \quad (52)$$

Because the partial systems are connected in cascade and both are matched, the scattering matrix  $S'$  of the complete system is matched also while its transmission coefficient is simply the product of the transmission coefficients of the partial junctions. Thus we have

$$S' = \begin{pmatrix} 0 & \beta'_n \delta'_{n_0-n} \\ \beta'_n \delta'_{n_0-n} & 0 \end{pmatrix}. \quad (53)$$

By inserting eqs (50) and (52) in eq. (53) we find for the absolute value of the transmission coefficient  $t_n$  of the complete system

$$|t_n| = |\beta'_n \delta'_{n_0-n}| = \frac{1}{2} |\sin \frac{1}{2} n_0 \vartheta + \sin (\frac{1}{2} n_0 - n) \vartheta|. \quad (54)$$

Now the position of the partition can be varied so that this system forms, indeed, a variable attenuator. The attenuation, referred to the transmission through the instrument with the partition on the extreme left ( $n = n_0$ ), is given by

$$\left| \frac{t_n}{t_0} \right| = \frac{1}{2} \left| 1 + \frac{\sin (\frac{1}{2} n_0 - n) \vartheta}{\sin \frac{1}{2} n_0 \vartheta} \right|. \quad (55)$$

It is, of course, desirable that the minimum attenuation should be zero, i.e.  $|t_0| = 1$ . If this condition for complete power transfer, eq. (32), is fulfilled, eq. (55) simplifies to

$$\left| \frac{t_n}{t_0} \right| = |t_n| = \cos^2 \frac{1}{2} n \vartheta, \quad n_0 \vartheta = \pi. \quad (56)$$

It is evident that the curve relating attenuation to the position of the thin partition is of a discontinuous nature. In order to obviate this undesirable feature in the actual instruments, a long wedge of absorbing material extending over several junctions is used instead of the partition which was assumed to be short in the idealized theory. The curve is then smoothed out and  $n$  in eqs (55) and (56) can be regarded as a continuous variable, proportional to the coordinate specifying the position of the wedge.

In the instrument shown in fig. 5.9, which is intended for use in the 3-cm wavelength band, the slots of the directional junctions have dimensions as given in fig. 5.5. From table 5.1 it follows that the number  $n_0$  to satisfy eq. (32) for total power transfer must be equal to 18.

Equations (55) and (56) indicate infinite attenuation for  $n = n_0$ . Now it is evident that the maximum attenuation obtainable in practice is determined by the properties of the wedge, which up till now was assumed to be completely absorbing. In the actual models built, the maximum

attenuation, measured with the wedge right up in output lead (4), fig. 5.8, is over 40 db. On the other hand for settings of attenuation well under 40 db the properties of the wedge are relatively unimportant.

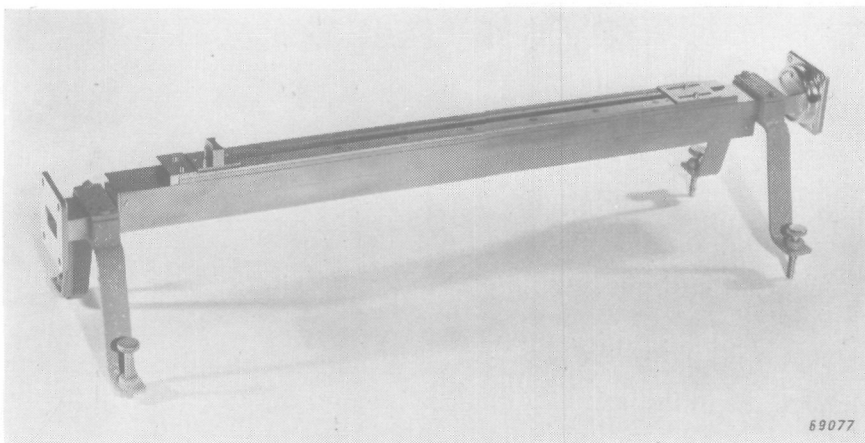


Fig. 5.9. Variable attenuator.

From eq. (53) it is clear that the instrument is matched irrespective of the value of  $n$ , i.e., the position of the wedge. This is only true if the directivity is perfect and the wedge matched. By careful design this ideal can be closely approximated and measurements indicate that the input standing-wave ratio can be kept below 1·1 in the frequency range between 8600 and 9600 Mc/s.

In the preceding section it was shown that the coupling of a system obeying the condition for total power transfer is broadband. This implies that the insertion loss  $t_0$  of the attenuator is independent of frequency, which fact is confirmed by measurements. Broadband coupling does not, however, insure insensitivity to frequency of the calibration curve, as differentiation of eq. (55) with respect to  $\vartheta$  demonstrates. To indicate the nature of this effect eq. (55) has been plotted in fig. 5.10 on a logarithmic scale for  $n_0 = 18$  and three values of  $\vartheta$ . The centre curve corresponds to the ideal case of eq. (56) with  $n_0\vartheta = 180^\circ$ . The point  $n = \frac{1}{2}n_0$ ,  $|t_n/t_0| = \frac{1}{2}$  is seen to be independent of  $\vartheta$  and hence of frequency. The calibration curves taken on actual models fit the theoretical curves very closely. The cross-over point is found to lie slightly higher than indicated in fig. 5.10. Possibly this is due to the wedge, the length of which was assumed to be very small in the theory.

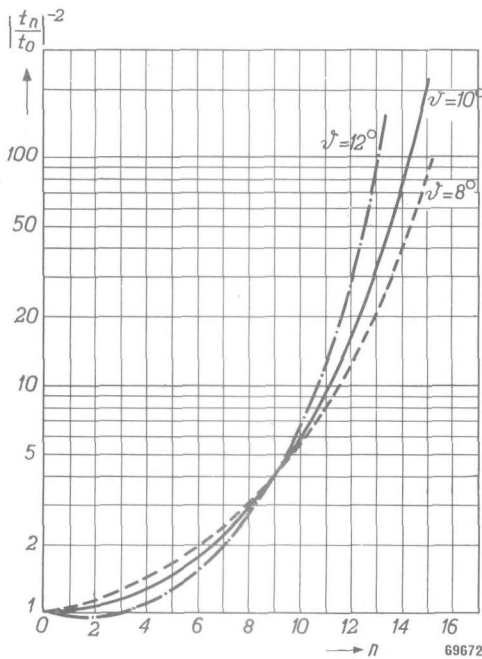


Fig. 5.10. Theoretical calibration curves for the variable attenuator. The spread in the values of  $\theta$  has been exaggerated for the sake of clarity.

## V. 6. Standard matching transformer

A directional coupler with equal power division is equivalent to a Magic Tee<sup>1)</sup>. Now it is known that by insertion of movable plungers in the side arms and a non-reflecting termination in the H-arm of a Magic Tee both phase and magnitude of the reflection suffered by a signal incident in the E-arm can be controlled at will through all possible values<sup>24)</sup>. It must be possible to achieve the same effect with the aid of a directional coupler giving equal power division.

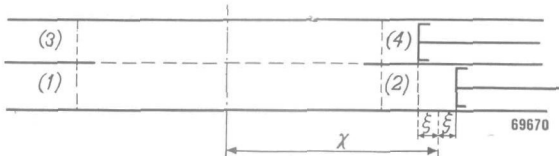


Fig. 5.11. Waveguide system used as a standard matching transformer.

Let us consider the system shown diagrammatically in fig. 5.11. It comprises a directional coupler with movable plungers inserted in leads (2)

and (4). Let their reflection coefficients referred to the symmetry plane of the coupler be denoted by  $g_2$  and  $g_4$  respectively. If directivity is assumed to be perfect the behaviour of the coupler is described in the usual notation by

$$\begin{pmatrix} b_1 \\ b_2 \\ b_3 \\ b_4 \end{pmatrix} = \begin{pmatrix} 0 & \beta & 0 & \delta \\ \beta & 0 & \delta & 0 \\ 0 & \delta & 0 & \beta \\ \delta & 0 & \beta & 0 \end{pmatrix} \begin{pmatrix} a_1 \\ a_2 \\ a_3 \\ a_4 \end{pmatrix}. \quad (57)$$

By substitution of the conditions

$$a_2 = g_2 b_2, \quad a_4 = g_4 b_4, \quad (58)$$

in eq. (57) the scattering matrix for the complete structure having only two output leads, numbered (1) and (3) in fig. 5.11, is found to be

$$\mathbf{S} = \begin{pmatrix} \beta^2 g_2 + \delta^2 g_4 & \beta\delta(g_2 + g_4) \\ \beta\delta(g_4 + g_2) & \delta^2 g_2 + \beta^2 g_4 \end{pmatrix}, \quad (59)$$

This matrix takes a particularly simple form if the directional coupler satisfies the condition for equal power partition, viz.

$$|\beta| = |\delta|, \quad n\vartheta = \pi/2. \quad (31)$$

By eq. (31) we have in this case

$$\beta = \frac{1}{2}(i+1), \quad \delta = \frac{1}{2}(i-1). \quad (60)$$

Elimination of  $\beta$  and  $\delta$  from eq. (59) with the aid of eq. (60) yields

$$\mathbf{S} = \frac{1}{2} \begin{pmatrix} i(g_2 - g_4) & -(g_2 + g_4) \\ -(g_2 + g_4) & -i(g_2 - g_4) \end{pmatrix}. \quad (61)$$

The form of the elements of  $\mathbf{S}$  now obtained suggests the introduction of the phase angles  $\chi$  and  $\xi$ , as shown in fig. 5.11, to specify the location of the plungers. The angle  $\chi$  corresponds to the distance between the reference plane of  $S$  and the median plane between the two plungers. The angle  $2\xi$  corresponds to the distance between the two plungers. For lossless plungers we have

$$g_2 = e^{2i(\chi+\xi)}, \quad g_4 = e^{2i(\chi-\xi)}. \quad (62)$$

The scattering matrix  $S$ , eq. (61), can now be written as a function of  $\chi$  and  $\xi$  only. Thus finally

$$\mathbf{S} = \begin{pmatrix} -\sin 2\xi e^{2i\chi} & -\cos 2\xi e^{2i\chi} \\ -\cos 2\xi e^{2i\chi} & \sin 2\xi e^{2i\chi} \end{pmatrix}. \quad (63)$$

Equation (63) clearly fulfils the general requirements imposed on the scattering matrix of a lossless junction. If  $\xi$  and  $\chi$  are considered as variables,

it is clear that the elements of  $\mathbf{S}$  can attain all possible values. But the most important point to note is the fact that the magnitude of the elements is a function of  $\xi$  only, whilst their phase angles are controlled independently by  $\chi$ . It is here that the superiority for this application of the directional coupler over the Magic Tee becomes apparent. The scattering matrix of a Magic Tee with plungers in its arms, it is true, may be brought in the form of eq. (63) by the introduction of suitable coordinates for the plunger positions. But the two plungers are physically spaced wide apart so that it is difficult to realize a mechanical drive for the separate control of  $\xi$  and  $\chi$ . In our case the two plungers are adjacent and the required mechanism is quite simple as is shown in fig. 5.12.

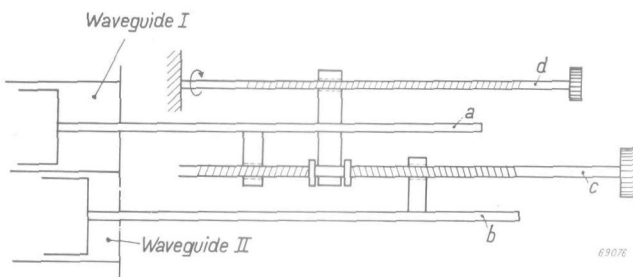


Fig. 5.12. Outline of the plunger drive needed for separate control of  $\xi$  and  $\chi$ .

The advantages of an instrument which allows separate control of modulus and argument of its reflection coefficient are evident. In microwave measurement work the diagram most often used is a polar plot of reflection coefficients. The controls of the instrument hence correspond to the natural coordinates of this diagram. Especially in measurements involving the plotting of lines of constant value of certain quantities, such as power or frequency, on the reflection-coefficient diagram (Rieke-diagram) such an instrument is highly desirable.

There are two methods to measure unknown reflection coefficients with the instrument. The first consists in its use as a variable standard termination. A matched load is connected to lead (3). The reflection coefficient  $\Gamma$  looking into lead (1) is then given by

$$\Gamma = -\sin 2\xi e^{2ix}. \quad (64)$$

Hence if the scale readings of the controls are calibrated in terms of  $\xi$  and  $\chi$ , the reflection coefficient  $\Gamma$  is known and it can be compared with the unknown reflection by known bridge methods.

In the other measuring method the instrument is used as a standard matching transformer. Then the termination of which the reflection coef-

ficient is to be determined is connected to output lead (3). The condition for a match in lead (1) under these circumstances will now be derived. Let the unknown reflection coefficient be denoted by  $g_3$ . Then

$$a_3 = g_3 b_3. \quad (65)$$

The reflection coefficient in lead (1), found by insertion of eq. (65) in eq. (63), is given by

$$\frac{b_1}{a_1} = \frac{g_3 e^{2ix} - \sin 2\xi}{e^{-2ix} - g_3 \sin 2\xi}. \quad (66)$$

Hence the condition for a match on the input side of the instrument is

$$g_3 = \sin 2\xi e^{-2ix}. \quad (67)$$

By comparison of eq. (67) with eq. (63) it can be concluded that the input lead is matched if the reflection coefficient looking into the output lead is complex conjugate to the reflection coefficient of the termination. This theorem applies to any lossless transformer, as by a suitable choice of reference planes the scattering matrix of such a structure can always be brought into the form of eq. (63). For the determination of  $g_3$  the same calibration of the controls can be used as before with the only difference that the sign of the phase angle should be reversed.

An actual model of the instrument for use in the 3-cm wavelength band is shown in fig. 5.13. It is composed of nine directional junctions of the type shown in fig. 5.5, which number gives equal power division (cf. table 5.1). The phase of the reflection coefficient is set by the large annular knob, while its modulus is controlled by the knob on the extreme right.

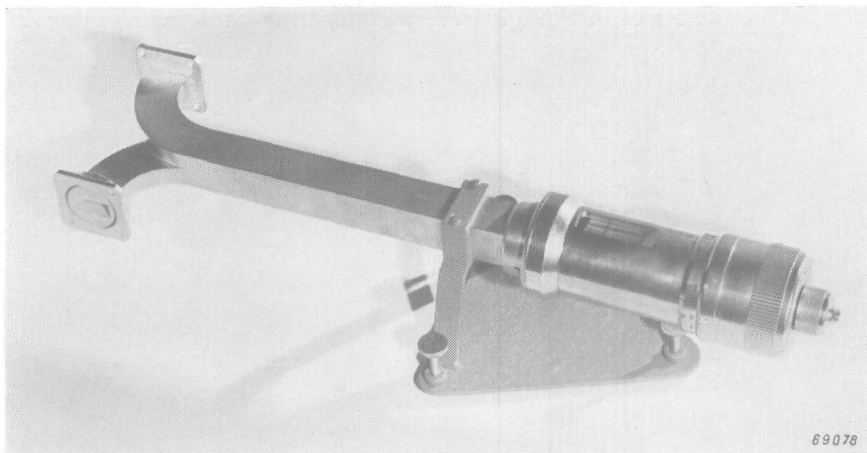


Fig. 5.13. Standard matching transformer.

The application of the instrument as a standard termination and a standard matching transformer is illustrated by figs 5.14 and 5.15 respectively. In the first case the instrument is terminated by a matched load and connected with its input lead to one of the side arms of a double Tee. The circuit element of which the reflection coefficient is to be measured is connected to the other side arm. The indication for the proper setting of the controls of the standard termination is zero signal in the H-arm of the double Tee. This arm is connected to a measuring receiver. It is to be noted that it is not necessary here to use a *Magic Tee* as bridge element.

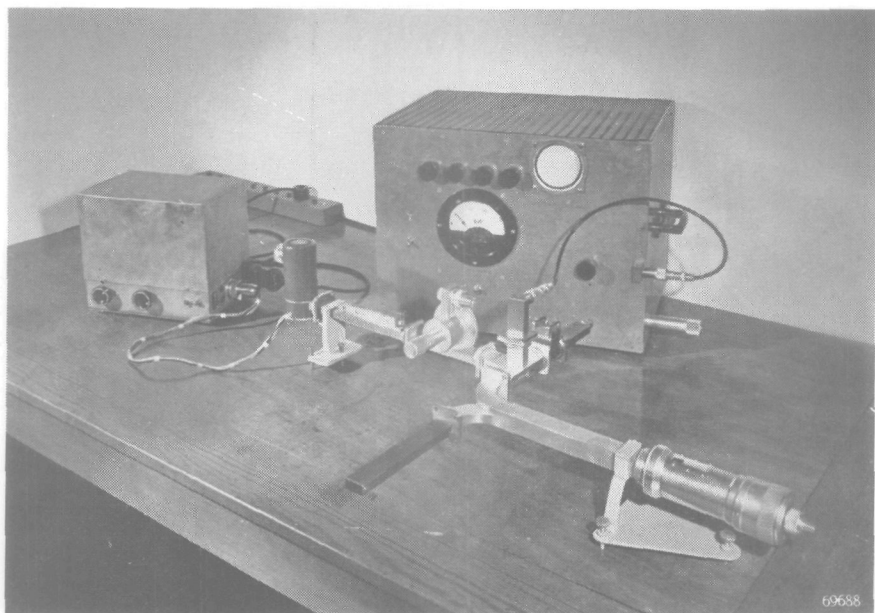


Fig. 5.14. Measurement of a reflection coefficient by comparison with the reflection of a standard termination.

In fig. 5.15 the circuit element to be measured forms the termination of the standard matching transformer. A directional coupler is used for the indication of the reflected wave, which must vanish for the proper setting.

The precision plunger drive with which the instrument is equipped enables us to measure accurately the directivity of the system of slots. To show this we shall derive the condition imposed on the plunger positions, i.e.  $g_2$  and  $g_4$ , for total decoupling of the input lead (1) from the output lead (3). If in the equation

$$B = SA, \quad (68)$$

where  $S$  is given by eq. (1), the conditions

$$a_2 = g_2 b_2, \quad a_3 = 0, \quad b_3 = 0, \quad a_4 = g_4 b_4, \quad (69)$$

are inserted, it follows from the resulting secular equation that

$$\frac{g_2 + g_4}{1 + g_2 g_4} = \frac{a}{a^2 - \beta\delta} = \frac{s_1 + s_2}{1 + s_1 s_2}. \quad (70)$$

If directivity is perfect ( $a = 0$ ), eq. (70) requires  $g_2 + g_4 = 0$ , in agreement with eq. (61). We now assume that  $a$  is small compared with unity and that

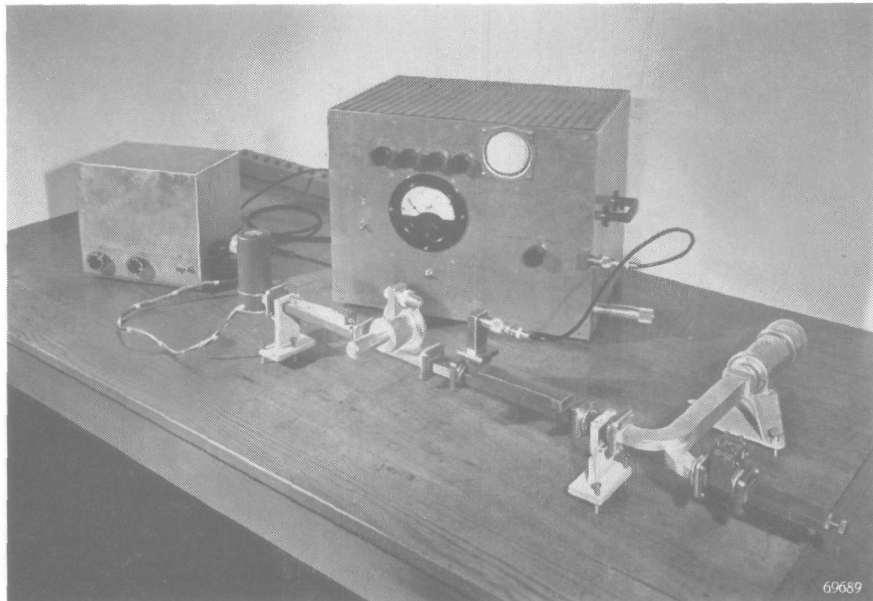


Fig. 5.15. Measurement of a reflection coefficient with the aid of a standard matching transformer.

$\beta$  and  $\delta$  differ little from the ideal values given by eqs (60). The right-hand side of eq. (70) is real and to the first order equal to  $2a$ . Expressing  $g_2$  and  $g_4$  in terms of  $\chi$  and  $\xi$  according to eqs (61) we obtain from eq. (70)

$$\cos 2\xi = 2a \cos 2\chi. \quad (71)$$

In this equation  $\chi$ , controlled by the “phase knob” of the matching transformer, is to be regarded as the independent variable. The procedure for the determination of  $a$  then consists in taking, for several values of  $\chi$ , the reading of  $\xi$  that decouples the output lead from the input. For small values of  $a$  a graph of  $2\xi$  against  $2\chi$  obtained in this way will show a

sinusoidal fluctuation of  $2\xi$  about  $\frac{1}{2}\pi$ . The amplitude of this sine curve is equal to  $a$ . This method for the measurement of  $a$  is closely related to the so-called S-curve method used for the determination of the characteristics of lossless transformers<sup>2), 6), 25)</sup>. This is brought out even more closely by writing eq. (71) in the form

$$\tan(\chi - \xi) = \frac{1 + 2a}{1 - 2a} \cotan(\chi + \xi). \quad (73)$$

It can be shown by an analysis of the behaviour of the matching transformer for  $a$ ,  $\beta$  and  $\delta$  differing slightly from their ideal values that the possible error in the reading for the modulus of the reflection coefficient depends mainly on the directivity and not so much on the coupling. Deviation of the latter quantity from its ideal value causes, apart from phase errors, only a reduced accuracy for low values of  $|\Gamma|$ . The possible error due to finite directivity, on the other hand, attains for  $|\Gamma| = \frac{1}{2}\sqrt{2}$  a maximum value which is equal to the directivity itself. As a directivity of 40 db has been realized in actual models, the corresponding absolute accuracy of  $|\Gamma|$  is  $\pm 0.01$ . Summarizing we may state that the standard matching transformer is best suited for measurements in the range  $0.1 < |\Gamma| < 1.0$ . For the accurate measurement of small reflections conventional apparatus such as a standing-wave detector or a squeeze section are to be preferred.

## CHAPTER VI. RESONANT SLOTS

In this chapter we shall extend the treatment of the type of junction discussed in the previous chapter so as to include resonant coupling. The literature on this subject<sup>26)</sup> is scanty, whereas extensive theoretical and experimental material is available on both resonant slots connecting the interior of a waveguide with outside space<sup>26), 27)</sup> and on resonant diaphragms across a section of rectangular waveguide<sup>28)</sup>.

### VI. 1. Single slots

In the preceding chapter it was shown that  $s_2$  is unaffected by the presence of a longitudinal slot in the wide side common to two rectangular waveguides. The properties of the slot are completely specified by the value of  $s_1$ . A transverse slot, on the other hand, leaves  $s_1$  undisturbed; its behaviour can be described fully by  $s_2$ .

A slot in the wall of a waveguide may be regarded as a magnetic dipole. If its length becomes of the order of half a wavelength it will accordingly display resonance effects.

We shall first treat the case of two sections of rectangular waveguide coupled by a single *longitudinal* slot in their common wide side, as shown in fig. 6.1. As  $s_2$  is equal to its unperturbed value —1, the scattering coefficients are given by

$$a = \gamma = \delta = \frac{1}{4}(s_1 - 1), \quad \beta = \frac{1}{4}(s_1 + 3), \quad (1)$$

as follows from the general equations (V. 3).

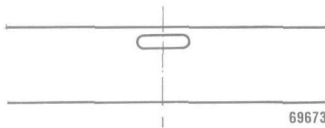


Fig. 6.1. Resonant longitudinal slot.

In Chap. II the expression for the reflection coefficient of a resonant termination has been derived. The quantity  $s_1$  which describes the behaviour of a resonant longitudinal slot is essentially a reflection coefficient, so that eq. (II.36) applies. The off-resonance reflection is given in this equation as  $i$ . The unperturbed (i.e. off-resonance) value of  $s_1$ , referred to the symmetry plane of the junction, has been found to be +1, however. Hence, in order to represent  $s_1$  correctly, equation (II.36) must be multiplied by  $-i$ , corresponding to an inward shift of the reference plane over a distance of a quarter wavelength. Thus we have

$$s_1 = 1 - \frac{2Q_L}{Q_E(1 - 2iQ_L \Delta\omega/\omega_0)}. \quad (2)$$

To simplify the discussion we will, for the moment, assume the junction to be lossless. Then

$$Q_E = Q_L \equiv Q. \quad (3)$$

In general this assumption introduces considerable discrepancies between theory and experiment. For resonant slots, however, it is often a useful approximation because of the heavy loading due, in our case, to the four output leads of the junction. Substituting eq. (3) in eq. (2) and introducing the phase angle of  $s_1$  we have

$$s_1 = e^{i\vartheta_1} = -\frac{1 + 2iQ \Delta\omega/\omega_0}{1 - 2iQ \Delta\omega/\omega_0}. \quad (4)$$

Hence

$$\tan \frac{1}{2} \vartheta_1 = -\frac{\omega_0}{2Q \Delta\omega}. \quad (5)$$

The introduction of  $\vartheta_1$  in eqs (1) yields

$$|a|^2 = |\gamma^2| = |\delta|^2 = \frac{1}{4} \sin^2 \frac{1}{2} \vartheta_1, \quad |\beta|^2 = 1 - \frac{3}{4} \sin^2 \frac{1}{2} \vartheta_1. \quad (6)$$

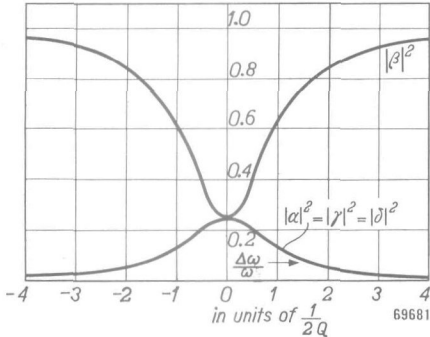


Fig. 6.2. Power-scattering coefficients of a single slot.

These power-scattering coefficients are plotted in fig. 6.2 against frequency according to eqs (5) and (6). At the resonance frequency we have by eqs (1) and (4)

$$\Delta\omega = 0, \quad s_1 = -1, \quad a = \gamma = \delta = -\frac{1}{2}, \quad \beta = +\frac{1}{2}. \quad (7)$$

The resonance scattering by a longitudinal slot is illustrated in fig. 6.3.

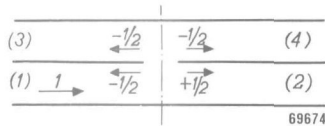


Fig. 6.3. Resonance scattering by a lossless longitudinal slot.

If the internal losses are accounted for by a finite value of  $Q_U$ , the scattering coefficients at the resonance frequency are found to be by eqs (1) and (2)

$$\Delta\omega = 0, \quad s_1 = -1 + \frac{2Q_L}{Q_U}, \quad a = \gamma = \delta = -\frac{1}{2}(1 - \frac{Q_L}{Q_U}), \quad \beta = \frac{1}{2}(1 + \frac{Q_L}{Q_U}). \quad (8)$$

A transverse slot, as shown in fig. 6.4, does not affect  $s_1$ . Substitution of the unperturbed value  $s_1 = +1$  in eqs (V.3) yields

$$a = \gamma = -\delta = \frac{1}{4}(1 + s_2), \quad \beta = \frac{1}{4}(3 - s_2). \quad (9)$$

In the vicinity of the resonance frequency of the slot,  $s_2$  is given by the

expression for the reflection coefficient of a resonant termination, eq. (II.36). Because the off-resonance value of  $s_2$  equals  $-1$ , the expression must be multiplied by  $i$ , corresponding to an inward shift of the reference plane over a distance of three-quarter wavelength. Thus

$$s_2 = -1 + \frac{2 Q_L}{Q_E (1 - 2i Q_L \Delta\omega/\omega_0)}. \quad (10)$$

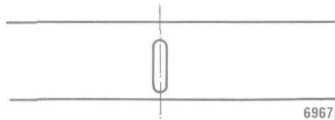


Fig. 6.4. Resonant transverse slot.

Assuming again for the moment the junction to be lossless we have

$$s_2 = -e^{i\vartheta_2} = \frac{1 + 2i Q \Delta\omega/\omega_0}{1 - 2i Q \Delta\omega/\omega_0}, \quad (11)$$

whence

$$\tan \frac{1}{2} \vartheta_2 = -\frac{\omega_0}{2Q \Delta\omega}. \quad (12)$$

The frequency dependence of the phase angles  $\vartheta_1$  and  $\vartheta_2$  of a longitudinal and a transverse slot respectively is given by the same function as is evident from eqs (5) and (12). The dependence of the absolute value of the scattering coefficients on the phase angle is also the same in both cases, so that fig. 6.2 applies to a transverse slot as well. The phase of the waves scattered by a transverse slot differs, however, from the phase of the waves scattered by a longitudinal slot. At resonance we have for a transverse slot

$$\Delta\omega = 0, \quad s_2 = +1, \quad a = \beta = \gamma = +\frac{1}{2}, \quad \delta = -\frac{1}{2}, \quad (13)$$

which situation is illustrated in fig. 6.5.

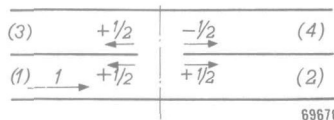


Fig. 6.5. Resonance scattering by a lossless transverse slot.

From eqs (7) and (13) it follows that in lossless junctions containing either a longitudinal or a transverse slot resonance is characterized by the scattering of one quarter of the incident power into each of the four output leads.

If the dissipation within the junction is included in the calculation, the scattering coefficients at resonance are given by

$$\Delta\omega = 0, s_2 = 1 - \frac{2Q_L}{Q_U}, \delta = \gamma = -\delta = \frac{1}{2}(1 - \frac{Q_L}{Q_U}), \beta = \frac{1}{2}(1 + \frac{Q_L}{Q_U}). \quad (14)$$

The strength of the coupling between the slot and the fields in the waveguides, as expressed quantitatively by  $Q_E$ , is determined mainly by the position of the slot relative to the axes of the waveguides. Clearly the lowest values of  $Q_E$  can be expected with slots cut in a position where the component of the undisturbed magnetic field parallel to the slot attains its maximum value. From fig. 4.1 it can thus be seen that for longitudinal slots in the wide side the minimum value of  $Q_E$  is achieved by slots adjacent to the narrow side. Transverse slots, on the other hand, display low values of  $Q_E$  if the slot is located in a central position. These effects are shown schematically in fig. 6.6.

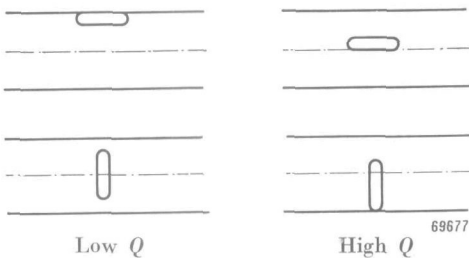


Fig. 6.6. Dependence of  $Q_E$  on slot position.

The dependence of the quality factor on slot width is only slight. Both the coupling of the slot to the fields in the waveguides and the energy-storing capacity of the slot increase with slot width. The net effect is a slow decrease of  $Q_E$  with increasing slot width.

Variation of the wall thickness affects only the energy stored in the slot, so that  $Q_E$  increases with the wall thickness. It should be realized, however, that the theory holds strictly only for an infinitely thin wall between the two sections of waveguide.

The general relation between the resonant frequency of a slot and its size, position and the dimensions of the waveguides is not easily accessible to theoretical treatment. This is even more so for slots filled with a dielectric material which differs from the dielectric within the waveguides. For the time being one can do little else but collect enough experimental material in order to be able to predict the slot dimensions needed in a specific case.

## VI. 2. Measurements on single slots

The three quantities specifying the behaviour of a single slot, either longitudinal or transverse, are  $\omega_0$ ,  $Q_L$  and  $Q_U$ . They may be determined experimentally by measuring the absolute value of  $a$ ,  $\beta$ ,  $\gamma$  or  $\delta$  as a function of frequency. If  $Q_L/Q_U$  is small compared with unity, however, the determination of  $Q_U$  by this method requires very high accuracy in the measurements, as follows from eqs (8) and (14). We have therefore developed an alternative procedure, which yields  $Q_L$  and  $Q_U$  with about the same accuracy.

The waveguide system used for the measurement is shown schematically in fig. 6.7. A generator  $G$  is connected to lead (1) of the junction and a receiver  $R$  to output lead (2). The frequency of the generator is variable;

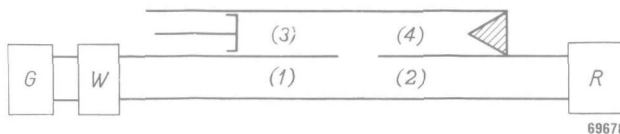


Fig. 6.7. Outline of the waveguide system used for the measurement of slot constants.  $G$  = generator,  $W$  = wavemeter,  $R$  = matched receiver.

its value can be determined with the aid of the wavemeter  $W$ . In output lead (3) a movable plunger has been inserted, whilst lead (4) is terminated by a matched load. It is evident that the value of the transmission coefficient  $b_2/a_1$  between lead (1) and lead (2) of this system depends on the position of the plunger in lead (3). By moving the plunger we can find a maximum and a minimum of the absolute value of this transmission coefficient. The measurement consists in the determination of the ratio of these two extreme values of  $|b_2/a_1|$ .

We shall now derive the equations needed for the interpretation of the measurements. The conditions to be inserted in the four equations contained in

$$\mathbf{B} = \mathbf{SA}, \quad (15)$$

are given by

$$a_2 = 0, \quad a_3 = g_3 b_3, \quad a_4 = 0. \quad (16)$$

Here  $g_3$  represents the reflection coefficient of the plunger ( $|g_3| = 1$ ). Substituting eq. (16) in eq. (15) and solving for  $b_2$  we obtain

$$\frac{b_2}{a_1} = 1 + \frac{\beta - 1}{1 - ag_3}. \quad (17)$$

In the derivation of eq. (17) nothing special has been assumed about the

junction except its symmetry. The transmission coefficient  $b_2/a_1$  is related to  $g_3$  by a bilinear transformation. Because  $g_3$ , as a function of the plunger position, describes a circle (in fact the unit circle) in the complex plane, the locus of  $b_2/a_1$  is a circle also. The centre of the latter is located at the point  $(\beta - |a|^2)/(1 - |a|^2)$ ; its radius equals  $|a||\beta - 1|/(1 - |a|^2)$ . Hence the extreme values of  $|b_2/a_1|$  are given by

$$\left| \frac{b_2}{a_1} \right|_{\max} = \left| \frac{\beta - |a|^2}{1 - |a|^2} \right| + \frac{|a| |\beta - 1|}{1 - |a|^2}, \quad (18)$$

$$\left| \frac{b_2}{a_1} \right|_{\min} = \left| \frac{\beta - |a|^2}{1 - |a|^2} \right| - \frac{|a| |\beta - 1|}{1 - |a|^2}. \quad (19)$$

The ratio  $H$  between these quantities is thus found to be

$$\left( \frac{|b_2|_{\max}}{|b_2|_{\min}} \right)_{a_1=\text{const}} = \frac{|\beta - |a|^2| + |a| |\beta - 1|}{|\beta - |a|^2| - |a| |\beta - 1|} \equiv H. \quad (20)$$

We now suppose that the only discontinuity in the common wide side between the two sections of waveguide is a single slot. From eqs (1), (2), (9) and (10) it follows that the expressions for  $|a|$  and  $\beta$  as functions of frequency and the slot constants are the same for both longitudinal and transverse slots, viz.

$$|a| = \frac{Q_L}{2Q_E |1 - 2i Q_L \Delta\omega/\omega_0|}, \quad \beta = 1 - \frac{Q_L}{2Q_E (1 - 2i Q_L \Delta\omega/\omega_0)}. \quad (21)$$

There is no need to derive explicitly the rather intricate expression for  $H$  as a function of frequency. It is sufficient to calculate  $H$  for two special values of  $\Delta\omega$ . At resonance  $H$  attains a maximum value, which is according to eqs (20) and (21) given by

$$\Delta\omega = 0, \quad H_{\text{res}} = \frac{1 + \frac{Q_L}{Q_U}}{\frac{Q_L}{Q_U} \left( 3 - \frac{Q_L}{Q_U} \right)}. \quad (22)$$

As the other special value of  $\Delta\omega$  we take the half-power points defined by

$$2 Q_L \frac{\Delta\omega}{\omega_0} = \pm 1. \quad (23)$$

For the corresponding expression  $H_{1/2}$  we find from eqs (20), (21) and (23)

$$H_{1/2} = \frac{\sqrt{\left(5 - \frac{Q_L}{Q_U}\right)^2 \left(1 + \frac{Q_L}{Q_U}\right)^2 + 4 \left(1 - \frac{Q_L}{Q_U}\right)^2} + \left(1 - \frac{Q_L}{Q_U}\right)^2}{\sqrt{\left(5 - \frac{Q_L}{Q_U}\right)^2 \left(1 + \frac{Q_L}{Q_U}\right)^2 + 4 \left(1 - \frac{Q_L}{Q_U}\right)^2} - \left(1 - \frac{Q_L}{Q_U}\right)^2}. \quad (24)$$

In figs 6.8 and 6.9  $H_{\text{res}}$  and  $H_{1/2}$  respectively are plotted as a function of  $Q_L/Q_U$ . In fig. 6.8 a graph is given also of the reciprocal of  $|b_2/a_1|_{\min}$  at the resonance frequency. The corresponding equation is obtained from eqs (19) and (21). Thus

$$\left| \frac{b_2}{a_1} \right|_{\min}^{-1} = \frac{1}{2} \left( 1 + \frac{Q_U}{Q_L} \right), \quad \Delta\omega = 0. \quad (25)$$

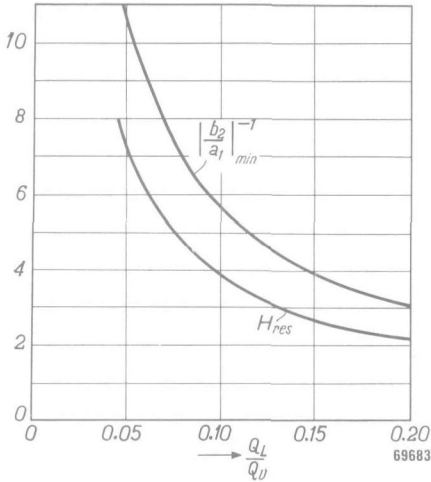


Fig. 6.8. The ratio  $H$  and the maximum insertion loss at the resonance frequency as a function of  $Q_L/Q_U$ .

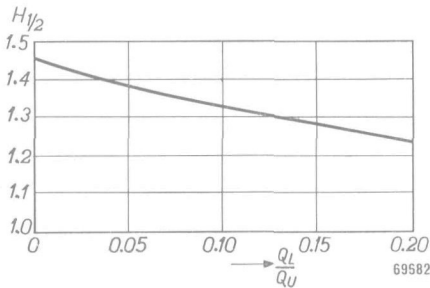


Fig. 6.9. The ratio  $H$  at half-power points as a function of  $Q_L/Q_U$ .

The measurement of this quantity, taken at the resonance frequency with a plunger setting so as to give maximum insertion loss, can be used conveniently as a check on the accuracy of the value of  $Q_L/Q_U$  calculated from the measured value of  $H_{\text{res}}$ .

A typical example of an experimentally determined plot of  $H$  against frequency is shown in fig. 6.10; the isolated point represents the maximum insertion loss. The measurements were taken on a junction having a single transverse glass-filled slot. The resonance frequency is seen to be 9070 Mc/s. The value of  $Q_L/Q_U$  corresponding to  $H_{\text{res}} = 3.45$  is read from fig. 6.8 to be 0.110. The value derived from a maximum insertion loss of 5.2

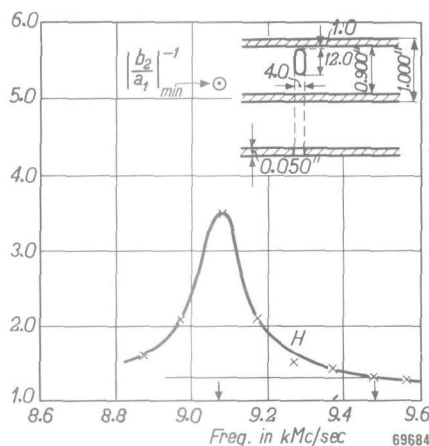


Fig. 6.10. Experimental plot for a transverse slot of  $H$  versus frequency. Slot dimensions in millimeters. The isolated point represents the maximum insertion loss at the resonance frequency.

is 0.106. Putting  $Q_L/Q_U = 0.108$  we derive from fig. 6.9 that  $H_{1/2}$  equals 1.32. Returning now to fig. 6.10 we deduce  $Q_L = 11.1$  and hence finally  $Q_U = 103$ .

A check on the symmetry of the junction may readily be achieved by an interchange of the positions of the plunger and the matched load in leads (3) and (4). The transmission coefficient  $b_2/a_1$  becomes under these conditions

$$\frac{b_2}{a_1} = 1 + \frac{\beta - 1}{1 - ag_4}, \quad (26)$$

where  $g_4$  denotes the reflection coefficient of the plunger now in lead (4). As the dependence of  $b_2/a_1$  on  $g_4$  is identical with its dependence on  $g_3$ , eq. (17), the measuring results should be the same in both cases.

### VI. 3. Resonant directional couplers

In Sec. V. 3 it has been proved that a lossless junction of rectangular waveguides having both a longitudinal and a transverse slot in the common wide side, as shown in fig. 5.4, constitutes a directional coupler. For perfect directivity the slot dimensions must be so as to make

$$s_1 + s_2 = 0. \quad (27)$$

This equation is satisfied if the phase angles  $\vartheta_1$  and  $\vartheta_2$  are equal. In the case of a lossless junction with resonant slots the phase angles are determined by eqs (5) and (12). Hence perfect directivity requires that

$$\left( \frac{\omega_0}{2Q\Delta\omega} \right)_1 = \left( \frac{\omega_0}{2Q\Delta\omega} \right)_2. \quad (28)$$

Subscripts 1 and 2 are used to distinguish between quantities referring to the longitudinal and the transverse slot respectively. It follows from eq. (28) that perfect directivity is maintained irrespective of frequency if both the quality factor and the resonant frequency are the same for the two slots. Let us assume this to be the case. Then we have (cf. eq. (V. 30))

$$a = \gamma = 0, \quad |\beta|^2 = \cos^2 \frac{1}{2} \vartheta, \quad |\delta|^2 = \sin^2 \frac{1}{2} \vartheta, \quad (29)$$

where  $\vartheta$  denotes, as before, the common value of  $\vartheta_1$  and  $\vartheta_2$ . The appearance of the graphs of  $|\beta|^2$  and  $|\delta|^2$  as a function of frequency is very much like the curves in fig. 6.2. The vertical scale must be taken differently, however, for  $|\beta|^2$  is zero and  $|\delta|^2$  equals 1 at the resonance frequency. This means that complete power transfer takes place in a resonant directional coupler at the resonance frequency. The power transfer, as a function of frequency, drops on both sides of the resonance frequency. A resonant directional coupler thus constitutes a branching filter.

An interesting application of the structure just described is its use as a radar duplexer. Let us consider the system shown in fig. 6.11. Let a signal of frequency equal to the resonance frequency of the directional coupler

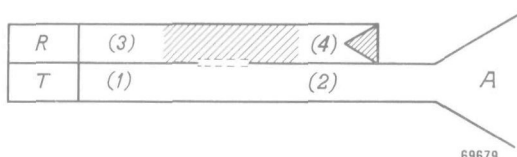


Fig. 6.11. Application of a resonant directional coupler as a radar duplexer.

enter the aerial  $A$ . It will travel down lead (2) towards the junction. There it is transferred completely to lead (3), thus reaching the receiver  $R$  irrespective of the terminations of leads (1) and (4).

A high-power pulse leaving the transmitter  $T$  will, in passing the junction, build up a high voltage across the slots. If now the upper section of waveguide contains a suitable gas filling, which is confined to that space by gas-tight dielectric layers in the slots, the high voltage will fire the gas. The ionized gas short-circuits the slots, thereby impeding the passage of the pulse towards lead (4). Hence the pulse leaves the system by lead (2) and the aerial. After the pulse the gas deionizes, so that the path from the aerial towards the receiver is open again for reflected pulses.

The main advantage of the system just described over duplexers of conventional design lies in the way it handles the spike. By the spike is meant that part of the transmitter pulse which passes through the gas-filled space before ionization starts. It can be seen from fig. 6.11 that the spike travels down lead (4) and is absorbed harmlessly by the matched load, whereas in conventional systems the spike reaches the receiver with the inherent danger of damage to it.

In actual models the slots are fitted with glass windows in order to ensure a gas-tight partition between the two sections of waveguide. For an accurate description of the behaviour of the junction it is then no longer justified to neglect dissipation.

In general the condition for a matched junction,  $\alpha = 0$ , ensures perfect directivity only if the junction is lossless. But in our case, because symmetry guarantees  $\alpha = \gamma$ , the same condition is still sufficient if dissipation takes place. If, accordingly, the general expressions for  $s_1$  and  $s_2$ , eqs (2) and (10), are inserted in the directivity condition, eq. (27), it follows that for broadband directivity all three relevant quantities, viz.  $\omega_0$ ,  $Q_L$  and  $Q_U$ , must have the same values for the two slots. Let us assume this to be the case. Then we have

$$\alpha = \gamma = 0, \quad \beta = 1 - \frac{Q_L}{Q_E (1 - 2i Q_L \Delta \omega / \omega_0)}, \quad \delta = - \frac{Q_L}{Q_E (1 - 2i Q_L \Delta \omega / \omega_0)}. \quad (30)$$

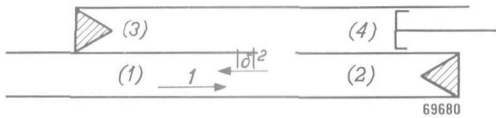


Fig. 6.12. Measurements of the insertion loss.

The quantity specifying the behaviour of the "cold" duplexer, i.e. as far as received signals are concerned, is the insertion loss. This can be measured in a very direct way as shown in fig. 6.12. It is evident, that with leads (2) and (3) terminated by matched loads the absolute value of the reflection coefficient in lead (1) caused by a plunger in lead (4) equals

$|\delta|^2$ . But this is just the fraction of the power entering the aerial (fig. 6.11) that reaches the receiver. In an analogous way we can measure the other power-scattering coefficient,  $|\beta|^2$ , by interchanging the terminations of leads (2) and (4). In the ideal case of slots with identical properties the expressions for  $|\beta|^2$  and  $|\delta|^2$  as a function of frequency are according to eq. (30) given by

$$|\beta|^2 = \frac{\left(\frac{Q_L}{Q_U}\right)^2 + \left(2 Q_L \frac{\Delta\omega}{\omega_0}\right)^2}{1 + \left(2 Q_L \frac{\Delta\omega}{\omega_0}\right)^2}, \quad |\delta|^2 = \frac{Q_L^2}{Q_E^2 \left\{1 + \left(2 Q_L \frac{\Delta\omega}{\omega_0}\right)^2\right\}}. \quad (31)$$

In fig. 6.13 measured values of  $|\beta|^2$  and  $|\delta|^2$  are shown for a junction with two resonant slots. The dimensions of the transverse slot are the same as of the single slot shown in fig. 6.10. By measurements on single longitudinal

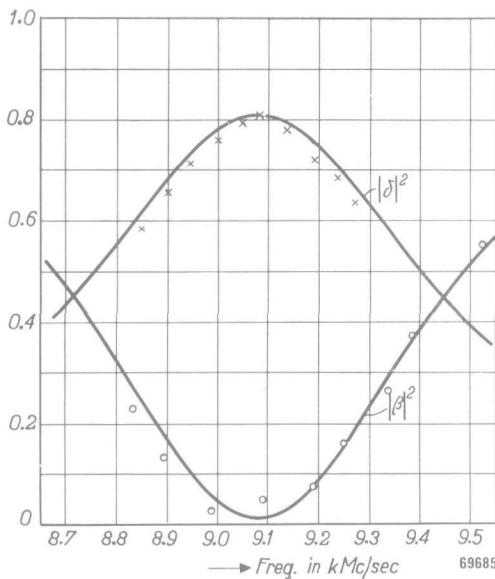


Fig. 6.13. Power-scattering coefficients of a radar duplexer versus frequency. The crosses and circles are experimental, the curves are theoretical.

slots the size was determined of the slot with as nearly as possible the same value of the slot constants as the transverse slot. The curves in fig. 6.13 have been calculated from eqs (31) after insertion of the constants of the transverse slot, as recorded in the preceding section.

REFERENCES

- 1) C. G. Montgomery, R. H. Dicke and E. M. Purcell, Principles of microwave circuits, McGraw-Hill, New York, 1948, Chap. 12.
- 2) J. C. Slater, Rev. mod. Phys. **18**, 441-512, 1946.
- 3) S. Tomonaga, J. phys. Soc. Japan **2**, 158-171, 1947; **3**, 93-104, 1948.
- 4) D. M. Kerns, J. Res. Bur. Stand. **42**, 515-540, 1949.
- 5) S. A. Schelkunoff, Electromagnetic waves, van Nostrand, New York, 1943, p. 35.
- 6) G. B. Collins, Microwave magnetrons, McGraw-Hill, New York, 1948, Chap. 5.
- 7) W. Altar, Proc. Inst. Radio Engrs **35**, 355-361; 478-484, 1947.
- 8) D. M. Kerns, J. Res. Bur. Stand. **46**, 267-278, 1951.
- 9) J. Rosenthal and G. M. Murphy, Rev. mod. Phys. **8**, 317-346, 1936.
- 10) E. Bauer, Introduction à la théorie des groupes et à des applications à la physique quantique, Presses universitaires, Paris, 1933.
- 11) H. Eyring, J. Walter and G. E. Kimball, Quantum chemistry, Wiley & Sons, New York, 1944.
- 12) J. A. Schouten, Tensor analysis for physicists, Clarendon Press, Oxford, 1951.
- 13) H. A. Bethe, Phys. Rev. **66**, 163-182, 1944.
- 14) H. A. Bethe, Radiation Laboratory Report 43-22.
- 15) H. A. Bethe, Radiation Laboratory Report 43-27.
- 16) H. J. Riblet, Proc. Inst. Radio Engrs **35**, 1307-1313, 1947.
- 17) J. Hessel, G. Goubaud and L. R. Battersby, Proc. Inst. Radio Engrs. **37**, 990-1000, 1949.
- 18) C. G. Montgomery, R. H. Dicke and E. M. Purcell, Principles of microwave circuits, McGraw-Hill, New York, 1948, Chap. 9.
- 19) M. Surdin, J. Inst. electr. Engrs **93**, III A, 725-736, 1946.
- 20) C. G. Montgomery, Technique of microwave measurements, McGraw-Hill, New York, 1947, Chap. 14.
- 21) P. E. Krasnushkin and R. B. Khokhlov, J. Techn. Phys. (Russian) **19**, 931-942, 1949.
- 22) H. J. Riblet and T. S. Saad, Proc. Inst. Radio Engrs **36**, 61-64, 1948.
- 23) S. Rosen and J. T. Bangert, Proc. Inst. Radio Engrs **27**, 393-401, 1949.
- 24) H. G. Beljers and W. J. van de Lindt, Philips Res. Rep. **6**, 96-104, 1951.
- 25) N. Marcuvitz, Waveguide handbook, McGraw-Hill, New York, 1951, pp. 132 et seq.
- 26) W. H. Watson, The physical principles of waveguide transmission and antenna systems, Clarendon Press, Oxford, 1947.
- 27) A. F. Stevenson, J. appl. Phys. **19**, 24-38, 1948.
- 28) L. D. Smullin and C. G. Montgomery, Microwave duplexers, McGraw-Hill, New York, 1948, Sec. 3.10.

**Summary**

The description of the electromagnetic behaviour of microwave circuits with the aid of the scattering matrix is systematically developed. Special attention is paid to resonators. The basic results obtained by Tomonaga on this subject are elaborated to the point of practical usefulness. General considerations about the consequences of structural symmetry of microwave circuits lead up to an extensive discussion of junctions consisting of two parallel sections of rectangular waveguide having one of their sides in common. The theory for directional couplers obeying these symmetry requirements is derived. Two instruments, viz. an attenuator and a standard matching transformer, both having a directional coupler as basic unit, are described in detail. The last chapter, finally, deals with resonant directional couplers.

### Samenvatting

Het electromagnetische gedrag van microgolfnetwerken, samengesteld uit golfpijpen, trilholten e.d., wordt gewoonlijk beschreven aan de hand van een vervangingsschema. Dit laatste wordt opgebouwd gedacht uit reactanties en weerstanden, onderling verbonden door tweedraadsleidingen. Deze werkwijze is vooral aantrekkelijk voor eenvoudige circuits met een of twee uitgangen. Voor de behandeling van microgolfcircuits met drie of meer uitgangen werkt een vervangingsschema nauwelijks meer verhelderend. Het dient dan slechts als kapstok om de meetresultaten aan op te hangen. Het is derhalve gebruikelijk om op deze gevallen een andere beschrijvingswijze toe te passen. In plaats van stromen en spanningen in een golfpijp te definiëren voert men grootheden in, welke de amplitudines van invallende en uitgaande golven aangeven. De eigenschappen van het circuit, dat de toevoerleidingen verbindt, worden nu beschreven met reflectie- en transmissiecoefficienten betrokken op deze golven. Analog aan de impedantiematrix, in zwang in de gebruikelijke netwerktheorie, kunnen bovengenoemde coefficienten samengevat worden in de verstrooiingsmatrix.

Dit proefschrift behandelt microgolfcircuits met behulp van de verstrooiingsmatrix. In het eerste hoofdstuk worden enige algemene eigenschappen van deze matrix afgeleid direct uit de vergelijkingen van Maxwell. In een recent artikel heeft Tomonaga aangetoond, hoe ook het gedrag van resonatoren op elegante wijze beschreven kan worden met behulp van de verstrooiingsmatrix. In hoofdstuk II wordt Tomonaga's theorie uitgebreid; met een aantal voorbeelden wordt de bruikbaarheid ervan gedemonstreerd.

Vele microgolfcircuits uit de praktijk bezitten een zekere mate van structurele symmetrie. Naast de vergelijkingen van Maxwell vormt dit een belangrijk gegeven voor de specificatie van de eigenschappen van een circuit. Het aantal parameters benodigd voor de volledige beschrijving van een symmetrisch circuit is steeds geringer dan het aantal nodig voor de beschrijving van een overeenkomstig niet-symmetrisch circuit. Een theorie voor de analyse van de invloed van structurele symmetrie op het aantal onafhankelijke parameters van de strooimatrix is het eerst gegeven door Dicke. Onderlangs heeft Kerns deze methode wiskundig streng gefundeerd met behulp van groepentheorie. In hoofdstuk III is een inleiding tot dit onderwerp gegeven. Als toepassing ervan worden in het vierde hoofdstuk circuits met vier toevoerleidingen besproken, die tweevoudige vlakke symmetrie vertonen. Een speciaal geval doet zich voor bij systemen bestaande uit twee golfpijpen met rechthoekige doorsnede, waarvan de assen parallel lopen en die over hun gehele lengte een zijwand gemeenschappelijk hebben. De koppeling tussen de pijpen wordt teweeg gebracht door gaten of sleuven in deze gemeenschappelijke wand. De eigenschappen van circuits van deze aard, voorzover zij verfiesvrij zijn, worden bepaald door slechts twee reële parameters.

In de hoofdstukken V en VI worden een aantal toepassingen van de juist vermelde circuits gegeven. In het bijzonder wordt aandacht geschonken aan richtingskoppelingen en daaruit afgeleide instrumenten. Deze omvatten onder meer een verzwakker, een geïjkte instelbare transformator en een radarduplexer.

## STELLINGEN

1. De gebruikelijke benaderende berekening van de demping in een golfpijp van een, zich in een bepaalde trillingsvorm voortplantende, golf ten gevolge van het eindige geleidingsvermogen van de wanden levert in bijna alle gevallen de uitkomst, dat de dempingsconstante voor frequenties hoger dan een zekere eindige waarde onbeperkt met de frequentie toeneemt. Dit resultaat is op algemene physische gronden als onjuist te verwerpen.

2. Toepassing van een eendraadstransmissieleiding is minder aantrekkelijk dan soms in de literatuur wordt gesuggereerd.

H. Kaden, Arch. elekt. Uebertragung 5, 399 - 414, 1951.

3. Het is verklaarbaar, dat stellingen geponeerd door promovandi aan een Universiteit gemiddeld een meer polemisch karakter hebben dan die geponeerd door promovandi aan een technische hogeschool.

4. De technische hulpmiddelen, sedert kort beschikbaar in het micro-golfgebied, kunnen met vrucht toepassing vinden bij het aanschouwelijk onderricht in de physische optica.

5. Het derde en vierde postulaat betreffende de eigenschappen van een groep, zoals geformuleerd door van der Waerden, laten een foutieve interpretatie toe.

B. L. van der Waerden, Moderne Algebra, Ungar Publishing Co., New York, 1943, p. 13.

6. De berekening van de acoustische impedantie van een luidsprekerkast, zoals uitgevoerd door Meeker, Slaymaker en Merrill, berust op een foutieve grondslag.

Meeker, Slaymaker and Merrill, J. ac. Soc. Am. 22, 206 - 210, 1950.

7. Van de toepassing van physische effecten, oorspronkelijk ontdekt voor lichtgolven, op het gebied der microgolven en omgekeerd kunnen nog vele vruchtbare resultaten verwacht worden.

8. Het lijkt aannemelijk, dat microgolfspectroscopie een waardevol industrieel hulpmiddel zal worden.

9. Er bestaat geen reden te verwachten, dat golfpijpen zullen worden gebruikt voor transmissie van signalen over grote afstanden.

M. Jouguet, Câbles et Transm. 1, 133 - 153, 1947; 2, 257 - 284, 1948.

10. De door Bell afgeleide conditie voor minimum ruisgetal voor een triode, nl. dat "the source susceptance shall resonate with the cold input susceptance of the tube with the anode earthed" is onjuist.

R. L. Bell, Proc. Inst. Radio Engrs 39, 1059 - 1063, 1951.

11. Voor het meten van ruis veroorzaakt door de afsluiting van een golfpijp verdient het gebruik van een ontvanger, bestaande uit een directe detector met een gelijkspanningsversterker, de voorkeur boven het gebruik van een superheterodyne ontvanger.
12. Het is gewenst de student aan de Technische Hogeschool er van te doordringen, dat hij de specialisatie, door hem verworven tijdens zijn afstudeerwerk, niet moet zien als noodzakelijke basis voor zijn verdere loopbaan.
13. Voor studenten en pas afgestudeerde ingenieurs van de Technische Hogeschool, die in militaire dienst worden geroepen, heeft de huidige zeer lange duur der eerste oefening een nadelige invloed op hun keuze voor hun verdere loopbaan in het burgerleven.